

1 **Primary marine aerosol emissions from the Mediterranean Sea**  
2 **during pre-bloom and oligotrophic conditions: correlations to**  
3 **seawater chlorophyll-a from a mesocosm study**

4  
5 **A. N. Schwier<sup>1</sup>, C. Rose<sup>1</sup>, E. Asmi<sup>1,\*</sup>, A.M. Ebling<sup>2</sup>, W.M. Landing<sup>2</sup>, S. Marro<sup>3,4</sup>, M.-L.**  
6 **Pedrotti<sup>3,4</sup>, A. Sallon<sup>3,4</sup>, F. Iuculano<sup>5</sup>, S. Agusti<sup>5,6</sup>, A. Tsiola<sup>7</sup>, P. Pitta<sup>7</sup>, J. Louis<sup>3,4</sup>, C.**  
7 **Guieu<sup>3,4</sup>, F. Gazeau<sup>3,4</sup>, and K. Sellegri<sup>1</sup>**

8  
9 <sup>1</sup>Laboratoire de Météorologie Physique CNRS UMR6016, Observatoire de Physique du  
10 Globe de Clermont-Ferrand, Université Blaise Pascal, 63171 Aubière, France

11 <sup>2</sup>Department of Earth, Ocean, and Atmospheric Science, Florida State University, Tallahassee  
12 FL 32306-4520, USA

13 <sup>3</sup>Laboratoire d'Océanographie de Villefranche (LOV), CNRS UMR7093, Observatoire  
14 océanologique, 06230 Villefranche-sur-mer, France

15 <sup>4</sup>Sorbonne Universités, UPMC Univ Paris 06, UMR7093, LOV, Observatoire océanologique,  
16 06230 Villefranche-sur-mer, France

17 <sup>5</sup>Instituto Mediterráneo de Estudios Avanzados (IMEDEA CSIC-UIB), 07190 Esporles,  
18 Mallorca, Spain

19 <sup>6</sup>The UWA Oceans Institute and School of Plant Biology, University of Western Australia, 35  
20 Stirling Highway, Crawley 6009, Australia

21 <sup>7</sup>Hellenic Centre for Marine Research (HCMR), PO Box 2214, 71003 Heraklion, Crete,  
22 Greece

23  
24 \* now at: Finnish Meteorological Institute, P.O. Box 503, 00101, Helsinki, Finland

25  
26 Correspondence to: A.N. Schwier (a.schwier@opgc.univ-bpclermont.fr), K. Sellegri  
27 (k.sellegri@opgc.univ-bpclermont.fr)

28  
29  
30  
31  
32  
33  
34  
35  
36  
37  
38  
39  
40  
41

## 42 Abstract

43 The effect of ocean acidification and changing water conditions on primary (and secondary)  
44 marine aerosol emissions is not well understood on a regional or a global scale. To investigate  
45 this effect as well as the indirect effect on aerosol that changing biogeochemical parameters  
46 can have,  $\sim 52 \text{ m}^3$  pelagic mesocosms were deployed for several weeks in the Mediterranean  
47 Sea during both winter pre-bloom and summer oligotrophic conditions and were subjected to  
48 various levels of  $\text{CO}_2$  to simulate the conditions foreseen in this region for the coming  
49 decades. After seawater sampling, primary bubble-bursting aerosol experiments were  
50 performed using a plunging water jet system to test both chemical and physical aerosol  
51 parameters (10-400nm). Comparing results obtained during pre-bloom and oligotrophic  
52 conditions, we find the same four log-normal modal diameters ( $18.5 \pm 0.6$ ,  $37.5 \pm 1.4$ ,  $91.5 \pm 2.0$ ,  
53  $260 \pm 3.2 \text{ nm}$ ) describing the aerosol size distribution during both campaigns, yet pre-bloom  
54 conditions significantly increased the number fraction of the second (Aitken) mode, with an  
55 amplitude correlated to virus-like particles, heterotrophic prokaryotes, TEPs, chlorophyll-a  
56 and other pigments. Organic fractions determined from kappa,  $\kappa$ , closure calculations for the  
57 diameter,  $D_p \sim 50 \text{ nm}$ , were much larger during the pre-bloom period (64%) than during the  
58 oligotrophic period (38%), and the organic fraction decreased as the particle size increased.  
59 Combining data from both campaigns together, strong positive correlations were found  
60 between the organic fraction of the aerosol and chlorophyll-a concentrations, heterotrophic  
61 and autotrophic bacteria abundance, and dissolved organic carbon (DOC) concentrations. As a  
62 consequence of the changes in the organic fraction and the size distributions between pre-  
63 bloom and oligotrophic periods, we find that the ratio of cloud condensation nuclei (CCN) to  
64 condensation nuclei (CN) slightly decreased during the pre-bloom period. The enrichment of  
65 the seawater samples with microlayer samples did not have any effect on the size distribution,  
66 organic content or the CCN activity of the generated primary aerosol. Partial pressure of  $\text{CO}_2$ ,  
67  $p\text{CO}_2$ , perturbations had little effect on the physical or chemical parameters of the aerosol  
68 emissions, with larger effects observed due to the differences between a pre-bloom and  
69 oligotrophic environment.

70

## 71 1. Introduction

72 With oceans covering 71% of the Earth's surface, sea spray aerosol comprises a large portion  
73 of the natural aerosol emissions, with an estimated contribution between 2,000 and 10,000 Tg  
74  $\text{yr}^{-1}$  for aerosols with diameter  $D_p < 20 \mu\text{m}$  (Gantt and Meskhidze, 2013). Marine aerosol can be

75 produced from primary processes (e.g. sea spray aerosol from breaking waves) and secondary  
76 processes (i.e. formation via chemical processing or gas-to-particle conversion). These  
77 aerosols can then have a large impact upon the Earth's radiative budget through both direct  
78 effects, such as light scattering, and indirect effects, by becoming cloud condensation nuclei  
79 (CCN) and affecting cloud formation and cloud properties (Novakov and Corrigan, 1996;  
80 Novakov and Penner, 1993). Due to the large flux of marine aerosol into the atmosphere, it is  
81 critical to better understand and determine the physical and chemical properties of marine  
82 aerosol as a function of changing marine environment water conditions.

83 At wind speeds greater than  $4\text{ m s}^{-1}$ , primary marine aerosol is primarily formed via bubble  
84 bursting from breaking waves; three main types of drops, film, spume and jet drops, are  
85 produced depending on the mechanism (Lewis and Schwartz, 2004). Based on the size of  
86 aerosol formed, the chemical composition ranges from primarily inorganic sea spray particles  
87 to particles rich in organic material, yet different studies have shown differing compositions  
88 over the same size range. Typically, particles of diameter  $D_p > 1\mu\text{m}$  have been found to be  
89 largely sea salt whereas smaller particles  $D_p < 1\mu\text{m}$  contain increasing concentrations of  
90 organics with decreasing diameter (Ault et al., 2013; Facchini et al., 2008; Keene et al., 2007;  
91 O'Dowd et al., 2004; Prather et al., 2013). For particles in the size range relevant to cloud  
92 formation (50-150nm), some have found an absence of hygroscopic salts in particles below  
93 200nm (Bigg and Leck, 2008), while other studies have shown the presence of sea salt and  
94 other inorganic elements (Ault et al., 2013; Clarke et al., 2006; Murphy et al., 1998; Quinn  
95 and Bates, 2011). Marine organic species remain largely uncharacterized (Benner, 2002) and  
96 organic concentrations can vary drastically throughout the water column, both temporally and  
97 spatially (Russell et al., 2010). Primary emissions can gain organics either as bubbles traverse  
98 through the water column or at the ocean surface from the organic rich microlayer (Barger and  
99 Garrett, 1970; Bigg and Leck, 2008; Blanchard, 1964; Blanchard and Woodcock, 1957;  
100 Garrett, 1967; Lion and Leckie, 1981; Matrai et al., 2008). The sea surface microlayer has  
101 been shown to exhibit physical, chemical and biological differences from oceanic subsurface  
102 water (Cunliffe et al., 2013).

103 The primary marine aerosol emission flux is characterized by different source functions, the  
104 number of aerosols by particle size by area by time (Lewis and Schwartz, 2004). These source  
105 functions are dependent on a number of physical parameters, dominated by wind speed and  
106 sea surface temperature, but are also affected by the sea state (wave height, shape, etc.) and  
107 salinity (Grythe et al., 2014). Aerosol emissions are also dependent on the chemical

108 composition of the seawater due to the presence of a rich and varied mixture of organic  
109 material. These organics can affect the waters' ability to form whitecaps (Callaghan et al.,  
110 2012) and change bubble lifetime (Garrett, 1967). Large-scale marine aerosol source functions  
111 used in models have started to include seawater composition (Langmann et al., 2008;  
112 Spracklen et al., 2008; Vignati et al., 2010) by focusing on parameterizations of the  
113 correlation between surface water chlorophyll-a (chl<sub>a</sub>) concentrations and aerosol organic  
114 fractions (O'Dowd et al., 2008; Rinaldi et al., 2013).

115 Previous studies have indicated changing size distribution with increasing organic material  
116 (Fuentes et al., 2010b; King et al., 2012; Sellegri et al., 2006). Sellegri et al. (2006) saw a log-  
117 normal mode amplitude shift towards smaller diameters with the addition of sodium dodecyl  
118 sulfate (SDS) to artificial seawater; Fuentes et al. (2010b) observed similar behavior in tests  
119 with artificial seawater and biogenic exudates, while King et al. (2012) saw an additional  
120 lognormal mode at 200nm with the addition of organic material to artificial seawater. Water  
121 temperature has also shown an effect on aerosol size distribution and number concentration,  
122 though different groups have seen varying trends. Mårtensson et al. (2003) saw increasing  
123 number concentrations for particles >350nm and decreasing concentrations for particles  
124 <70nm with increasing water temperature in measurements of synthetic seawater. For all  
125 diameters in between, there was no clear trend. Sellegri et al. (2006) compared artificial  
126 seawater at 4° and 23°C and found that the lognormal modal diameters all decreased with  
127 decreasing water temperature. Zábory et al. (2012b) measured the size distribution of NaCl  
128 and succinic acid/NaCl aerosol produced from an impinging water jet over a temperature  
129 range from 0 - 16°C and found that the temperature did not influence the size distribution, yet  
130 it did influence the magnitude of aerosols produced (increasing temperatures led to decreased  
131 aerosol production). The dominance of small particles (dry diameter 10-250nm) decreased  
132 with increasing water temperature over the range 0-10°C. Above 10°C, total number  
133 concentrations were stable regardless of the temperature. Similar results were found testing  
134 winter Arctic Ocean water (Zábory et al., 2012a) and Baltic seawater (Hultin et al., 2011),  
135 though for the Baltic seawater, the number concentration continued to drop until a water  
136 temperature of ~14°C.

137 Concentrations of marine organic aerosol seem to be highly dependent on the biological  
138 productivity at the ocean surface, following a seasonal bloom cycle. Studies performed at  
139 Mace Head in the North Atlantic Ocean and Amsterdam Island in the Southern Indian Ocean  
140 determined that the organic concentrations as well as the organic:sea salt ratio were highest in

141 the spring/summer and the lowest in the winter (Sciare et al., 2000, 2009; Yoon et al., 2007).  
142 Phytoplankton blooms lead to increased levels of organic material (OM), both dissolved and  
143 particulate (Ducklow et al., 1995), with dissolved organic carbon (DOC) concentrations often  
144 greater than 80 $\mu$ M under bloom conditions (Hansell et al., 2009). Different studies have  
145 linked the total submicron organic mass fraction of sea spray aerosol to chl<sub>a</sub> levels observed  
146 by satellite (Albert et al., 2012; O'Dowd et al., 2008; Rinaldi et al., 2013; Vignati et al., 2010);  
147 other studies have shown that the organic mass fraction was correlated with dimethylsulfide  
148 (DMS) (Bates et al., 2012) or heterotrophic bacteria abundance (Prather et al., 2013) instead.  
149 Hultin et al. (2010) measured seawater at depths of 2m during an ocean cruise west of Ireland  
150 and did not observe a correlation between chl<sub>a</sub> and sea spray production, instead finding a  
151 relationship with dissolved oxygen. Rinaldi et al. (2013) found that the correlation between  
152 chl<sub>a</sub> and OM at Mace Head was higher than the correlation of colored dissolved organic  
153 material or seawater particulate organic carbon; however, the optimum correlation between  
154 chl<sub>a</sub> and OM was observed with an eight day time lag for chl<sub>a</sub>, indicating a complex, indirect  
155 relationship between biological processes and transferable organic matter. Various studies  
156 have shown linear correlations between chl<sub>a</sub> concentrations and organic fraction (O'Dowd et  
157 al., 2008; Rinaldi et al., 2013); others have observed exponential fitting correlation (Gantt et  
158 al., 2011), a power fit correlation (Fuentes et al., 2011), or a Langmuir functional relationship  
159 correlation (Long et al., 2011).

160 The CCN activity of marine aerosol has been tested in various laboratory experiments.  
161 Fuentes et al. (2010a) determined a plunging water jet system to be the bubble generation  
162 method most representative of ambient marine aerosol. In a separate study, Fuentes et al.  
163 (2010b) collected seawater samples from the West African coast for CCN measurements with  
164 phytoplankton exudates and saw a shift towards higher number concentrations and smaller  
165 diameters in samples with high biological material. They found a variable relationship  
166 between chl<sub>a</sub> concentrations and OM production, stating that organic enrichment might also  
167 be dependent on specific conditions of algal blooms. The same dataset showed an increase in  
168 critical supersaturation of 5-24% for the samples with high biological material compared to  
169 artificial seawater (Fuentes et al., 2011). Moore et al. (2011) performed laboratory  
170 experiments with NaCl or artificial seawater in combination with SDS, *Synechococcus*,  
171 *Ostreococcus* or oleic acid and found that 100 $\times$  the normal organic concentration still did not  
172 affect the CCN activity or cloud formation properties. King et al. (2012) tested artificial  
173 seawater with different organics (palmitic acid, sodium laurate, fructose, mannose, SDS) and

174 found that the number concentration decreased with the presence of stronger surfactants, most  
175 likely due to surface layer stabilization. The CCN activity was dependent on the contribution  
176 of the varying salts in the particle phase rather than the organics. In recent wave channel  
177 experiments with natural seawater, Prather et al. (2013) saw the activation diameter augment  
178 from 63 to 118nm after a five-fold increase in bacteria abundance; the size distributions  
179 remained essentially unchanged (as did phytoplankton, chl<sub>a</sub> and total organic carbon (TOC)  
180 abundances and concentrations), leading to the notion that a change in the sea spray chemical  
181 composition (the number fraction mode) must have affected the activation diameter. During  
182 the same campaign, Collins et al. (2013) observed the hygroscopicity parameter,  $\kappa$ , reduce by  
183  $86\pm 5\%$  over the same time period as the bacterial increase.

184 The production of organic matter in oceanic surface water is expected to be substantially  
185 modified in the coming decades as a consequence of climate change and ocean acidification  
186 (Doney et al., 2012). Ocean acidification is defined as the increase in ocean acidity and  
187 associated changes in seawater chemistry, due to the absorbance of a very significant amount  
188 of anthropogenic CO<sub>2</sub> by the oceans ( $2.5 \pm 0.5$  Gt C or  $\sim 26.3\%$  of anthropogenic emissions,  
189 Le Quéré et al. (2014)). Since the beginning of the industrial era, the pH in ocean surface  
190 waters has already decreased by 0.1 units, on average, equivalent to an increased acidity of  
191 26%. Further acidification is expected by 2100, ranging from 0.06 to 0.32 units, equivalent to  
192 an increased acidity of 15 to 110%, depending on the considered CO<sub>2</sub> emission scenario  
193 (Ciais et al., 2013). Although it is well established that ocean acidification has the potential to  
194 significantly impact marine biological processes (see Riebesell and Tortell (2011) and  
195 Weinbauer et al. (2011) for a comprehensive review), it is still unclear how these changing  
196 biogeochemical water conditions will affect the properties and production of marine aerosols.  
197 Furthermore, the effect of such an acidification and consequently the resulting feedback on  
198 Mediterranean marine aerosol and the regional climate remains unknown.

199 Mesocosms are defined as experimental enclosures from one to several thousands of litres that  
200 maintain natural communities under close-to-natural conditions (Riebesell et al., 2013). They  
201 have been increasingly used in both aquatic and terrestrial ecology (Stewart et al., 2013),  
202 especially on the effects of environmental and/or anthropogenic disturbances on a large  
203 variety of chemical and biological processes. In the context of ocean acidification, mesocosms  
204 have been used on several occasions for experimental time periods spanning from a few days  
205 to a few weeks, and were found to be efficient in studying the effects of this driver over such  
206 short time scales (Riebesell et al., 2008, 2013). Archer et al. (2013) recently showed, during a

207 mesocosm experiment in the Arctic, that with seawater acidification and increased CO<sub>2</sub>  
208 concentrations, average concentrations of DMS decreased by up to 60% at the lowest pH.  
209 Inversely, concentrations of DMSP, the precursor to DMS, increased by up to 50%. In the  
210 remote ocean, DMS was predicted by modeling studies to be one of the main precursors for  
211 CCN in the marine boundary layer, and studies have shown that regional DMS emission  
212 changes could affect CCN sensitivity (Cameron-Smith et al., 2011; Woodhouse et al., 2013).

213 Many past mesocosm experiments which focused on the effects of ocean acidification have  
214 been performed in relatively eutrophic conditions or with nutrient addition initially or during  
215 the experiment. However, about 60% of the ocean surface is associated with low productivity,  
216 termed oligotrophic areas. Decreased nutrient availability and the expansion of low  
217 productivity regions are projected with increasing CO<sub>2</sub> concentrations, as enhanced thermal  
218 stratification is expected to lead to surface layer nutrient depletion (Irwin and Oliver, 2009;  
219 Polovina et al., 2008). Nutrient availability also might have strong effects on the community  
220 response to ocean acidification (Hare et al., 2007), so there is a clear need to evaluate the  
221 sensitivity of oligotrophic marine environments to this anthropogenic effect. The  
222 Mediterranean Sea is one of the most nutrient-poor waters in the world with maximum open  
223 sea area chlorophyll concentrations of 2-3mg m<sup>-3</sup>. Its trophic status varies from oligotrophic-  
224 mesotrophic in the northwestern basin to extremely oligotrophic in the eastern basin (Moutin  
225 and Raimbault, 2002; The Mermex Group, 2011). High biological activity occurs annually in  
226 parts of the western Mediterranean, including coastal France in the late winter and early  
227 spring (D'Ortenzio and Ribera d'Alcalà, 2009; Siokou-Frangou et al., 2010).

228 In this work, we collected water from three mesocosms deployed in the Northwestern  
229 Mediterranean Sea over two campaigns during different seasons as part of the European  
230 Mediterranean Sea Acidification in a changing climate (MedSeA; <http://medsea-project.eu>)  
231 and the Chemistry-AeRosol Mediterranean Experiment (ChArMEx) projects to test the effects  
232 of ocean acidification and changes in the biogeochemistry of the seawater on the physical and  
233 chemical properties of primary marine aerosol including size distributions and CCN activity.

## 234 2. Materials and Methods

### 235 2.1 Measurement sites and campaigns

236 Mesocosm experiments were performed during two intensive campaigns: the first, during  
237 summer oligotrophic conditions (hereafter referred to as non-bloom conditions), occurred

238 from 22 June to 10 July 2012 at the Station de Recherches Sous-marines et Océanographiques  
239 in the Bay of Calvi (BC), Corsica; the second, performed during winter pre-bloom conditions,  
240 took place from 21 February to 5 March 2013 in the Bay of Villefranche (BV), France. The  
241 two bays share many similarities in term of temperature, salinity, phosphate ( $\text{PO}_4^{3-}$ ),  
242 nitrate+nitrite ( $\text{NO}_x$ ), and silicate (Si) seasonal variations, and they both show typical bloom  
243 conditions in winter-spring and oligotrophic conditions in the summer, corresponding to a  
244 stratified water column. Pre-bloom conditions are also observed at both locations (Gazeau et  
245 al., submitted). The presence of pre-bloom and non-bloom conditions was confirmed by the  
246 order-of-magnitude difference in the average seawater chla concentrations ( $\text{chla}_{\text{BC,avg}} =$   
247  $0.069 \pm 0.009 \text{ mg m}^{-3}$ ,  $\text{chla}_{\text{BV,avg}} = 1.005 \pm 0.125 \text{ mg m}^{-3}$ ). Detailed site and experimental  
248 information for both campaigns that legitimize the comparison to test in these two locations at  
249 different seasons can be found in Gazeau et al. (submitted).

250 Briefly, the mesocosms used in this study (volume of  $\sim 52 \text{ m}^3$ ) were fully described in Guieu et  
251 al. (2014). The mesocosms consisted of large bags made of two 500- $\mu\text{m}$  thick films of  
252 polyethylene mixed with vinyl acetate (EVA, 19%) with nylon meshing in between to allow  
253 maximum resistance and light penetration (HAIKONENE KY, Finland). Natural seawater  
254 was filtered through a mesh grid to remove large debris when deploying the mesocosms. In  
255 order to avoid actual atmospheric deposition, the mesocosms were covered with UV-  
256 transparent ethylene tetrafluoroethylene (ETFE) roofs, except during periods of sampling. In  
257 this way, transfer of rainwater/deposition was prevented, while preserving the sunlight  
258 irradiance of the mesocosms. The covers were elevated to  $\sim 10 \text{ cm}$  above the top of the  
259 mesocosms, allowing air to circulate to avoid a confinement effect in the trapped water.  
260 Among nine deployed mesocosms, three remained unmodified as controls and six were  
261 modified in terms of partial pressure of  $\text{CO}_2$ ,  $p\text{CO}_2$ . The  $p\text{CO}_2$  levels used were slightly  
262 different between the two campaigns, as a consequence of different ambient  $p\text{CO}_2$  levels (i.e.  
263  $\sim 450$  vs.  $350 \mu\text{atm}$  at BC and BV, respectively). In the Bay of Calvi, the six targeted elevated  
264  $p\text{CO}_2$  levels were 550, 650, 750, 850, 1000 and  $1250 \mu\text{atm}$ . In the Bay of Villefranche, the  
265 levels were 450, 550, 750, 850, 1000 and  $1250 \mu\text{atm}$ . These elevated  $p\text{CO}_2$  levels were reached  
266 by adding varying volumes of  $\text{CO}_2$  saturated seawater to the mesocosms. At both sites,  
267 seawater was pumped from near the mesocosms and sieved onto a 5 mm mesh sieve in order  
268 to remove large organisms. Pure  $\text{CO}_2$  was actively bubbled through the water for several  
269 minutes in order to achieve saturation; the water was then transferred to 25L plastic containers  
270 for addition to the mesocosms. Depending on the targeted  $p\text{CO}_2$  level, 50L to more than 500L

271 were added. A diffusing system was used to ensure a perfect mixing of this CO<sub>2</sub> saturated  
272 seawater inside the mesocosms. In order to minimize the stress induced by the addition of  
273 large quantities of acidified water, the acidification of the mesocosms was performed over 4  
274 days, and the experiments started when the targeted *p*CO<sub>2</sub> levels were reached. The CO<sub>2</sub>  
275 levels were chosen in order to cover the range of atmospheric CO<sub>2</sub> concentrations projected  
276 for the end of the century following various scenarios (RCP 2.6 to RCP 8.5; (IPCC, 2013)).

277 For the experiments described here, every morning approximately 5L of surface water (taken  
278 within a 15cm depth from the surface) was pumped from each mesocosm using a  
279 perfluoroalkoxy alkane (PFA) pump (St-Gobain Performance Plastics) activated by the  
280 pressurized air from a diving tank and connected to braided PVC tubing (Holzelock-Tricoflex,  
281 I.D. 9.5mm). The water pump was flushed with seawater from the respective mesocosm prior  
282 to sampling. Samples were stored in large brown glass bottles outside (avoiding direct  
283 sunlight) until the experiments were performed that same day. During the BV campaign, the  
284 pump could not be used on 3 March 2013 due to unsafe sea conditions; water was instead  
285 manually sampled from the mesocosms with 2.5L glass bottles while wearing long gloves.  
286 Additionally, due to dangerous wind and wave conditions, sampling was not performed on 5  
287 March 2013 during the BV campaign. Instrumental failures occurred on 4 and 10 July 2012 at  
288 BC and on 28 February – 1 March 2013 at BV.

289 For both campaigns, the mesocosms were located off-shore in pelagic waters in order to  
290 measure primary marine aerosol properties and biogeochemical parameters of the water while  
291 minimizing contamination from anthropogenic sources. The mesocosms were reached via  
292 ocean kayak or boat. For both campaigns, sampling operations were performed from a mobile  
293 plastic platform that was moved via a rope network. The water temperature variances between  
294 BC and BV are quite drastic, given the time of year the experiments took place. From  
295 conductivity, temperature and depth (CTD) measurements, at BC the water temperature  
296 measured nearest to the surface varied from 21.8-25.2°C; at BV, the temperatures ranged from  
297 13.0-13.6°C.

298 For the experiments described here, we focused on three different mesocosms: control  
299 mesocosm C3, and acidified mesocosms P3 and P6. Mesocosm P6 was the most acidified of  
300 all mesocosms (*p*CO<sub>2</sub>~1250µatm), and P3 was acidified to an intermediate level  
301 (*p*CO<sub>2</sub>~750µatm). This allowed a range of acidification effects to be analyzed.

## 302 2.2 Experimental methods

303 Bubble-bursting experiments were performed using a square glass tank (20l×20w×25h cm<sup>3</sup>),  
304 filled with 3.6L of seawater (water depth of ~10cm), sealed with a stainless steel lid and  
305 continuously flushed with particle-free air (11LPM). The tank was constantly slightly over-  
306 pressured with particle-free air to ensure the absence of ambient room air. Aerosols were  
307 generated by splashing mesocosm seawater through plunging water jets, separated into 8 jets  
308 via a flow distributor. The mesocosm seawater was re-circulated using a peristaltic pump; to  
309 minimize an increasing temperature of the seawater caused by constant re-circulation, a  
310 stainless steel heat exchanger was used on the seawater exiting the pump. The temperature of  
311 the water was recorded with a temperature sensor at the beginning and end of each experiment  
312 (for the BV campaign). Since no measurements of the bubble size distribution could be  
313 performed in such a small device, all water flow characteristics were performed according to  
314 the Fuentes et al. (2010a) settings, to reproduce the same bubble size distribution. The water  
315 flowrate was set to 1.8LPM, the height of the jets above the water surface was 9cm and the  
316 penetration depth of the jets was ~7.5cm. Particle-free air was blown over the seawater (using  
317 a j-shaped tube ~1.5cm above the water surface) to mimic the wind blowing effect on the  
318 bubble-bursting process. Some of the water samples were also enriched by the addition of an  
319 organic rich microlayer from the same mesocosms (average 100mL, range 50-170mL). The  
320 enriched mesocosm samples were tested after the un-enriched sample to compare the effect of  
321 additional organic species.

322 Blank measurements were performed during the first ten minutes of each experiment by  
323 verifying the aerosol concentration was zero in the particle-free air flushed tank. Between  
324 each water sample testing, the aquarium and tubing were rinsed with ultrapure water  
325 (>18MΩ), and clean water was re-circulated throughout the experimental setup for 10-15  
326 minutes. Experiments were performed on the mesocosm water in different orders each day to  
327 make sure there were no experimental biases.

328 The aerosol flow was passed through a diffusion drier and was sent through a neutralizer into  
329 a differential mobility particle sizer (DMPS) and miniature continuous-flow streamwise  
330 thermal-gradient CCN chamber (CCNc) (Roberts and Nenes, 2005) to determine particle  
331 CCN activation properties. The neutralizer used was a variable-amplitude corona discharge  
332 which charges particles to the equilibrium charge distribution (Stommel and Riebel, 2004,  
333 2005). For the BC experiments, the neutralizer voltage was ~2.8kV and for BV, ~2.0kV.

334 For the CCNc-DMPS system, aerosol flow passed first through a TSI-type DMA (length  
335 44cm) selecting particle sizes in 26 channels ranging from 10-400nm by stepping the voltage  
336 over an integration time of about 8 ½ minutes. Immediately after the DMA, the aerosol flow  
337 was split between the CCNc and a TSI CPC model 3010. The DMA sheath flow rate was  
338 9LPM and the sample flow rate was 1LPM in BC; 7.5LPM and 1.35LPM was used in BV,  
339 respectively. For the BV campaign, the aerosol flow was split 1LPM for the CPC and  
340 0.35LPM to the CCNc. In the CCNc, a total aerosol flow rate of 100sccm with a sheath-to-  
341 aerosol flow ratio of 5 was used. The CCNc operated at specific temperature gradient (dT)  
342 settings, testing two different supersaturations (SS). For the BC campaign, a temperature  
343 gradient of 6°C (dT6) was used in the column and the top temperature of the column varied as  
344 the ambient temperature changed ( $T_{top} - T_{amb} = 2^{\circ}\text{C}$ ); in BV, dT6 and a temperature gradient  
345 of 3°C (dT3) were tested and the top temperature of the column was always set at 30°C. The  
346 data is plotted as activated fraction vs. particle diameter and fit with a sigmoid curve, from  
347 which we obtain the activation diameter at each dT (see Asmi et al. (2012) for more details).  
348 The CCNc system was calibrated with atomized  $(\text{NH}_4)_2\text{SO}_4$  and NaCl solutions at the  
349 beginning, end and throughout each campaign. The activation diameter of the calibration was  
350 then used to calculate the corresponding supersaturation; this supersaturation was then used  
351 for all mesocosm experiments. The activation diameters and corresponding supersaturations  
352 for each dT for both campaigns are shown in Table 1 (dT6=0.39% SS, dT3=0.08%). The  
353 range of SS values used in this work is typical of those reported in natural clouds. Anttila et  
354 al. (2009) found cloud SS values from 0.18 to 0.26% for low-level clouds in Northern  
355 Finland, Hegg et al. (2009) obtained a SS range from 0.2 to 0.3% for clouds over the  
356 California coast, and Asmi et al. (2012) found SS values from 0.1 to 0.3% at the puy-de-  
357 Dôme station in Central France.

### 358 2.3 Seawater parameters

359 Every day at 8:30 (local time), depth-integrated sampling (0 to 10m) was performed in each  
360 mesocosm using 5L Hydro-Bios integrated water samplers. Samples for pigment analyses  
361 were filtered (2L) onto GF/F. Filters were directly frozen with liquid nitrogen and stored at -  
362 80°C. Measurements were performed on an HPLC from filters extracted in 100% methanol,  
363 disrupted by sonication and clarified by filtration (GF/F Whatman). Samples for microbial  
364 diversity (2mL) were fixed with 0.5% final concentration glutaraldehyde, frozen in liquid  
365 nitrogen, and then transferred to a -80°C freezer. Virus-like particles, heterotrophic and  
366 autotrophic prokaryotes abundances were measured with the use of Flow Cytometry (Beckton

367 Dickinson FACS Calibur model). Total organic carbon (TOC) was measured instead of  
368 dissolved organic carbon (DOC) in order to avoid contamination during filtration. However,  
369 the TOC measurement is referred to hereafter as DOC, due to the low concentration of  
370 particulate organic carbon in both sites (averaged over all mesocosms and all sampling times,  
371 BC:  $4.32 \pm 0.91 \mu\text{Mol}$ , BV:  $11.49 \pm 5.50 \mu\text{Mol}$ , which was typically less than 10% of TOC)..  
372 DOC concentrations were determined on 20mL samples by high temperature oxidation with a  
373 Shimadzu 5000A TOC Analyzer. Transparent exopolymeric particles (TEPs) concentrations  
374 were measured spectrophotometrically according to a dye-binding assay (Engel, 2009).  
375 Samples (250mL) were filtered onto 0.4mm pore size polycarbonate filters under low vacuum  
376 ( $<100\text{mm Hg}$ ), stained with 1mL of Alcian blue solution (0.02g Alcian blue in 100mL of  
377 acetic acid solution of pH2.5) and rinsed with 1mL of distillate water. Filters were then  
378 soaked for 3h in 6mL of 80% sulfuric acid ( $\text{H}_2\text{SO}_4$ ) to dissolve the dye, and the absorbance of  
379 the solution was measured at 787nm, using acidic polysaccharide xanthan gum as a standard.

### 380 3. Results and Discussion

381 In studying the effects of ocean acidification, it was necessary to observe whether changes  
382 with biogeochemical processes affected primary marine aerosol emissions and chemical and  
383 physical aerosol properties. For many of the parameters studied (e.g. chl<sub>a</sub> concentrations, total  
384 prokaryotic cells and virus-like particles abundances), there were no strong discernible  
385 differences between the control, C3, or the acidified mesocosms, P3 and P6 along the course  
386 of the experiments; however, there were often large differences between the two campaigns  
387 due to the pre-bloom and non-bloom conditions. While several studies have shown the effects  
388 of ocean acidification on biogeochemical parameters in eutrophic waters (Galgani et al., 2014;  
389 Schulz et al., 2013), observations from the MedSea experiment showed no effect of ocean  
390 acidification on most of the biogeochemical parameters in these oligo- to mesotrophic areas.  
391 These results are discussed more fully in Gazeau et al. (submitted). As a consequence, we did  
392 not expect any impact on the primary marine aerosol physical aerosol properties. In the  
393 following sections, we will relate trends observed with different biogeochemical parameters to  
394 those observed in the primary marine aerosol.

#### 395 3.1 Aerosol Size Distributions and Number Concentration

396 The marine aerosol size distributions remained fairly stable during a given experiment, which  
397 lasted around one hour for each water sample. The aerosol size distribution also remained

398 stable throughout the course of each campaign, with a similar distribution shape. Four  
399 lognormal modes were fit to the average size distributions of each campaign, with results  
400 summarized in Fig. 1 and Table 2. The average size distributions were taken from 214 size  
401 distributions for BC and 182 size distributions for BV, and size envelopes are also included  
402 within Fig. 1. In order to investigate the size of the aerosol independently of the concentration,  
403 the size distributions were normalized using the total aerosol number concentration. We found  
404 that the primary marine aerosol size distributions were best described using the three expected  
405 modes: nucleation mode (around 20nm), Aitken mode (around 40nm), and accumulation  
406 mode (around 100nm); and an additional fourth mode around 260nm. Using only three modes  
407 for the fitting procedure could not satisfactorily represent the primary marine aerosol size  
408 distribution. A mode at around 300nm was also found by Sellegri et al. (2006) during  
409 bubbling experiments for which the effect of wind on the surface breaking bubbles was  
410 simulated in a similar experiment set-up. The 300nm mode was interpreted by the authors as  
411 the result of a thicker bubble film where the bubbles are forced to break by the wind instead of  
412 reaching a natural breaking thickness. The four average lognormal modal diameters  
413 determined ( $18.5 \pm 0.6$ ,  $37.5 \pm 1.4$ ,  $91.5 \pm 2.0$ ,  $260 \pm 3.2$ nm) were present in both BC and BV. The  
414 lognormal mode fitting was also used to determine the particle number fraction at each  
415 lognormal modal diameter. Looking at the number fractions on a daily temporal scale for  
416  $SS=0.39\%$ , the lognormal mode number fractions remained relatively constant throughout  
417 both campaigns, though differences were noted between the campaigns (Fig. 2, Table 2).  
418 Throughout the campaign in BC, the fractions of Modes 1-3 were approximately equal in  
419 magnitude (0.297), whereas in BV, the magnitude of the Mode 2 (the Aitken mode) fraction  
420 relative to the other modes was dominant (0.48). These same trends were observed for all  
421 experiments using  $SS=0.08\%$  and all the enriched mesocosm samples (Figs. 3-4). When  
422 augmenting the bacterial abundance in seawater, Collins et al. (2013) observed an increased  
423 particle fraction of the smallest lognormal mode diameter with no change to the shape or  
424 magnitude of the size distribution; this was attributed to the replacement of internally mixed  
425 salt/organic particle types by insoluble organic type particles. Previous studies have also  
426 indicated changing size distributions or mode number fractions with increasing organic  
427 material (Fuentes et al., 2010b; Sellegri et al., 2006). In the present study, we will examine  
428 which chemical component is linked to the increase of the Aitken mode particles in Section  
429 3.3.

430 Many other studies have found different lognormal mode distributions of both artificial and  
431 natural seawater samples, though many have similar modal sizes. Differences in the size  
432 distribution of laboratory generated primary marine aerosol found in the literature seem to  
433 depend on the method used to generate them. Fuentes et al. (2010a) observed 4 modes (modal  
434 sizes 14, 48, 124, 334nm) generated from plunging-water jet experiments with artificial  
435 seawater. Mode 4 was believed to be linked to splashing water from the jet mechanism.  
436 Plunging-water jet experiments were found to most closely mimic the size distribution of  
437 ambient primary marine aerosol (Fuentes et al., 2010a) while generating sufficient aerosol for  
438 characterization measurements. In a separate study (Fuentes et al., 2010b), 4 modes  
439 represented both artificial and natural seawater (modal sizes 15, 45, 125, 340nm) well. Similar  
440 to our findings, increasing organic content was found to increase the number fraction of Mode  
441 2 while decreasing the relative fractions of the other modes. In similar experiments with Baltic  
442 seawater collected between May and September, Hultin et al. (2011) observed either two  
443 lognormal modes (site: Askö, 86, 180nm) or three lognormal modes (site: Garpen, 93, 193,  
444 577nm). Selleagri et al. (2006) tested synthetic sea salt with a weir and observed 3 lognormal  
445 modes (4°C: 30, 85, 200nm; 23°C: 45, 110, 300nm). After adding SDS, they noticed an  
446 increase in the fraction of particles at the smallest lognormal diameter. In synthetic seawater  
447 experiments with sintered glass filters, Mårtensson et al. (2003) observed one submicron  
448 lognormal mode (100nm); Tyree et al. (2007) observed a lognormal mode at the same  
449 diameter using artificial and natural seawater with pore diffusers. The Mårtensson et al.  
450 (2003) and Tyree et al. (2007) studies using sintered glass filters or pore diffusers report  
451 relatively different size distributions compared to those obtained by plunging jet experiments,  
452 likely due to the bubble formation processes. Collins et al. (2013) observed three lognormal  
453 modes in seawater wave channel experiments (~90, 220, 1000nm), with changing number  
454 fractions as described in the above paragraph.

455 Temperature has also been shown to affect size distributions and aerosol number  
456 concentrations (Hultin et al., 2011; Mårtensson et al., 2003; Zábóri et al., 2012a). The initial  
457 and final water temperatures were measured over the course of an experiment (~1hr, BV  
458 only); the water temperature was found to increase by  $4.6 \pm 1.2^\circ\text{C hr}^{-1}$  on average due to the  
459 constant water recirculation through the peristaltic pump and an insufficient heat exchange  
460 system (encompassing all experiments, water temperatures ranged from ~11.7-26.8°C from  
461 the initial to final measurement). This increase is 2-5× times higher than the  $1\text{-}2^\circ\text{C hr}^{-1}$   
462 temperature increase measured by Zábóri et al. (2012a). Even with this large temperature

463 range, we did not observe that the increase in the water temperature affected the shape of the  
464 size distribution. We were not able to make qualitative statements about the relationship  
465 between the number concentration and temperature, with the level of uncertainty in the wind  
466 flow stability within these experiments. Acidification had no effect on the aerosol size  
467 distribution, as no clear differences were found between mesocosms C3, P3, and P6 within a  
468 given field campaign.

### 469 3.2 Activation Diameter

470 By testing two temperature gradients, it is possible to look at the hygroscopic properties of  
471 different size particles based on the different supersaturations at which they are activated. The  
472 activation diameter time series measured at SS=0.39% (dT6) is shown in Fig. 5. In BC, there  
473 is little variation temporally between the control and acidified mesocosms tested  
474 ( $D_{p,50,avg}=46.47\pm 0.88\text{nm}$ ), indicating that acidification does not have a large direct effect on  
475 CCN activity. Additionally, the enriched samples showed similar behavior to the non-  
476 enriched waters, indicating that the addition of the organic-rich microlayer had little effect on  
477 the water uptake for the aerosols. For the experiments incorporating the enriched microlayer,  
478 the entire organic-rich volume was added a few minutes before starting the water jet system,  
479 rather than being continuously introduced to the tank throughout the entire experiment. This  
480 could have led to microlayer depletion over the course of an experiment, explaining why no  
481 visible difference was seen between the enriched and un-enriched samples. However, no clear  
482 difference was seen between the first (when the microlayer was present) and subsequent size  
483 distributions during a given microlayer enriched experiment. In past experiments, the addition  
484 of organics to bubbling experiments have shown changes in the size distribution (Sellegrì et  
485 al., 2006), particle number concentration (Fuentes et al., 2010b; King et al., 2012; Tyree et al.,  
486 2007), and CCN activity (Collins et al., 2013; Fuentes et al., 2011). Other experiments have  
487 shown no visible change (Moore et al., 2011) from the addition of organics, similar to the  
488 experiments performed in this study. In some studies, the concentrations and/or nature of  
489 some of the organic surfactants were unrealistic (King et al., 2012; Moore et al., 2011;  
490 Sellegrì et al., 2006). At BV, the average activation diameter for SS=0.39% over the course of  
491 the experiments was  $D_{p,50,avg}= 59.48\pm 1.1\text{nm}$  (Fig. 5), while at SS=0.08% the average  
492 activation diameter was  $D_{p,50,avg}= 141.91\pm 10.8\text{nm}$  (Fig. 6). Activation diameters larger than  
493 the corresponding salt standards (here, shown as NaCl), indicating higher organic presence,  
494 are observed more at BV than BC for SS=0.39% due to the organic pre-bloom conditions,  
495 whereas the non-bloom water conditions were very stable at BC. For SS=0.08%, the

496 activation diameters are very similar to the NaCl standard, which signifies a lower organic  
 497 fraction for larger particles. Activation diameters for individual mesocosms in both campaigns  
 498 are shown in Table 3.

499 There is an anti-correlation of the activation diameter at SS=0.39% with the ambient average  
 500 air temperature in BV (Fig. 5), though no correlation exists with SS=0.08% (Fig. 6), or in BC  
 501 (Fig. 5). However, more daily temperature variance was observed in BV than BC, based on  
 502 the time of year of the campaigns. This anti-correlation could indicate an additional  
 503 temperature impact on the emission of small particles (~50nm) and their chemical  
 504 composition, though this effect is unclear and undocumented in the literature.

505 We investigated if the observed differences in the activation diameters from BC and BV could  
 506 be linked to the different operating techniques used for the campaigns. As indicated  
 507 previously,  $T_{top}$  in BC was variable, changing as the ambient temperature changed. As the  
 508 ambient temperature changed throughout the day, the temperature in the column would also  
 509 change, leading to possible temperature instabilities throughout the course of an experiment.  
 510 On the contrary, in BV,  $T_{top}$  was fixed at 30°C, a temperature higher than the daily  
 511 temperature variability. In this way, temperature fluctuations in the column were avoided.  
 512 However, in observing the measured temperatures throughout the column for both campaigns  
 513 and all the experiments, the temperatures of the column remained quite stable for both  
 514 methods of operation, so we believe that these effects are very minor. Additionally, it has  
 515 been shown that organics can volatilize in the CCN column due to the temperature gradient  
 516 (Asa-Awuku et al., 2009), biasing observed CCN activity. It is possible that this occurred for  
 517 both campaigns based on the relatively high measured operating temperatures observed in the  
 518 column; if organic material was volatilized, the activation diameters would increase from  
 519 those shown here.

### 520 3.3 Kappa and Organic Fraction

521 The hygroscopicity of the aerosol was determined using kappa-Köhler theory (Petters and  
 522 Kreidenweis, 2007) following Asmi et al. (2012). Using the activation diameter and numerical  
 523 iteration, the kappa value was determined when the maximum of the saturation curve was  
 524 equal to the supersaturation in the CCNc, following,

525

$$526 \quad S(D_p) = \frac{D_p^3 - D_{p,50}^3}{D_p^3 - D_{p,50}^3(1-\kappa)} \exp\left(\frac{4\sigma_w M_w}{RT \rho_w D_p}\right) \quad (1)$$

527  
 528 where  $S$  is the supersaturation,  $D_p$  is the diameter of the droplet,  $D_{p,50}$  is the dry diameter,  $R$  is  
 529 the gas constant,  $T$  is temperature, and  $\sigma_w$ ,  $M_w$ , and  $\rho_w$  are the surface tension, molecular  
 530 weight and density of water, respectively. Lower kappa values correspond to more  
 531 hydrophobic, or organic-like, particles. In BC, the average mesocosm kappa value at  
 532 SS=0.39% was  $\kappa_{\text{avg,BC}}=0.95\pm0.17$ , In BV, the average mesocosm kappa values for SS=0.39%  
 533 and 0.08% are  $\kappa_{\text{avg,BV}}=0.45\pm0.13$  and  $0.78\pm0.14$ , respectively. This indicates that the smaller  
 534 particles (measured at the higher SS) were higher in organic material. The kappa values  
 535 obtained at SS=0.08% are more representative of the kappa that would be obtained for a bulk  
 536 chemical composition, as most of the aerosol mass is comprised in the accumulation mode for  
 537 submicron particles. Our value then falls well into the suggested range of the kappa average of  
 538 marine aerosol,  $\kappa_{\text{marine}}=0.72\pm0.24$  (Pringle et al., 2010).. Little variance was seen between the  
 539 control and acidified mesocosms.

540 Using the calculated kappa values, we determined the organic fraction using a kappa closure  
 541 equation,

542

$$543 \quad \kappa_{\text{total}} = \varepsilon_{\text{org}}\kappa_{\text{org}} + (1 - \varepsilon_{\text{org}})\kappa_{\text{inorg}} \quad (2)$$

544

545 where  $\varepsilon_{\text{org}}$  is the bulk volume fraction of organic material and  $\kappa$  is the kappa of the organic or  
 546 inorganic material. Following Collins et al. (2013), we used  $\kappa_{\text{inorg}}=1.25$ , a good proxy for  
 547 seawater, and  $\kappa_{\text{org}}=0.006$ . In BC, the organic fraction ranged from -0.21 to 0.46 (average,  
 548  $0.24\pm0.14$ ) for SS=0.39%. For BV, the organic fraction ranged from 0.43-0.80 (average,  
 549  $0.64\pm0.11$ ) for SS=0.39% and 0.19-0.55 (average,  $0.38\pm0.11$ ) for SS=0.08%. Previous studies  
 550 have also found mass organic fractions ranging from 30-80% in sea spray aerosol studies of  
 551 water from the Northern Atlantic, Sargasso Sea near Bermuda, and Pacific water near La  
 552 Jolla, California (Collins et al., 2013; Facchini et al., 2008; Keene et al., 2007). Negative  
 553 organic fractions were calculated during the BC campaign due to the sensitivity of Eq. (2) to  
 554 the value of  $\kappa_{\text{inorg}}$  over  $\kappa_{\text{org}}$ . We show results here using a  $\kappa_{\text{inorg}}$  value supported by literature  
 555 rather than determine non-realistic  $\kappa_{\text{inorg}}$  values to provide positive organic fractions.  
 556 Therefore, the values shown in this work can be considered low estimates of the organic  
 557 fraction. Table 3 shows average kappa and organic fraction values of each mesocosm for both  
 558 campaigns.

559 The organic fraction of the Aitken mode particles (obtained from measurements performed at  
 560 SS=0.39%) is significantly increased during the BV experiment compared to the BC  
 561 experiment. This indicates that the Mode 2 fraction increase observed in the size distribution  
 562 is due to the presence of organic matter, in agreement with the observations of Collins et al.  
 563 (2013)

564 The ratio of cloud condensation nuclei (CCN) to condensation nuclei (CN) decreased slightly  
 565 during the pre-bloom period for SS=0.39%: at BC,  $CCN/CN_{average}=0.55\pm0.03$  whereas at BV,  
 566  $CCN/CN_{average}=0.45\pm0.07$ . The change between CCN/CN during the oligotrophic and pre-  
 567 bloom conditions was likely due to the combined effects of a higher organic fraction and  
 568 higher Mode 2 to Mode 1 ratio during pre-bloom conditions, likely caused by the increasing  
 569 organic content of the water due to the pre-bloom. For SS=0.08% measured at BV,  
 570  $CCN/CN_{average}=0.15\pm0.02$ .

### 571 3.4 Correlations with biological parameters

572 In a recent study, Rinaldi et al. (2013) showed that chla was the best biological surrogate for  
 573 predicting organic enrichment in sea spray. Chla parameterizations are currently being used in  
 574 models to account for the organic content of seawater. We find a strong linear correlation with  
 575 same-day measurements of organic fraction (from SS=0.39%) and total chla concentrations  
 576 ( $R^2=0.781$ ,  $p<0.00001$ ) shown in log-log scale in Fig. 7, following

$$577 \quad \text{Organic Fraction}[\%] = 42.28 \times (\text{chla})[\text{mg m}^{-3}] + 22.98 \quad (3)$$

578 Similar correlations were also found with a number of pigments: chlorophyll c1+c2  
 579 ( $R^2=0.783$ ,  $p<0.00001$ ), 19'-butanoyloxyfucoxanthin ( $R^2=0.711$ ,  $p<0.00001$ ), alloxanthin  
 580 ( $R^2=0.699$ ,  $p<0.00001$ ), sum carotenes ( $R^2=0.773$ ,  $p<0.00001$ ) and 19'-  
 581 hexanoyloxyfucoxanthin ( $R^2=0.736$ ,  $p<0.00001$ ) (Fig. 8). Various studies have found linear  
 582 correlations between the organic fraction of aerosols measured at a receptor site and chla  
 583 concentrations observed by satellite along the back-trajectory (Langmann et al., 2008;  
 584 O'Dowd et al., 2008; Rinaldi et al., 2013; Vignati et al., 2010); others have found exponential  
 585 fittings (Gantt et al., 2011) with the same methodology or a Langmuir functional relationship  
 586 (Long et al., 2011) using a model with experimental data from Facchini et al. (2008) and  
 587 Keene et al. (2007). Fig. 7 shows many of the existing chla-organic fraction parameterizations  
 588 in the literature, including this work. It is clear that many of the parameterizations from the  
 589 Northern Atlantic Ocean also describe the correlation in the Mediterranean Sea fairly well,

590 even though the methodologies for most of them are very different from the one used in this  
591 study. The parameterization derived in this work lays at higher organic content when  
592 compared to the other parameterizations, even though it does not include secondary organic  
593 contributions as do many of the satellite-receptor site studies. This is likely due to the size  
594 dependence of the organic fraction that we observed in the BV data. Our parameterization is  
595 applicable for Aitken mode type aerosols and would probably shift towards lower organic  
596 content for accumulation mode particles. It is also possible that organic components in  
597 Mediterranean primary marine aerosol are of multiple origins and not solely linked linearly to  
598 chl-a-rich species. Bacteria have also been observed to affect the organic material in seawater  
599 (Gruber et al., 2006; Jiao et al., 2010; Ogawa et al., 2001). We find a correlation with  
600 heterotrophic prokaryotes ( $R^2=0.476$ ,  $p=1.3\times 10^{-5}$ ), virus-like particles ( $R^2=0.161$ ,  $p=0.025$ ),  
601 autotrophic prokaryotes ( $R^2=0.499$ ,  $p<0.00001$ ) and *Synechococcus* abundance ( $R^2=0.143$ ,  
602  $p=0.033$ ), shown in Fig. 9A-D. In a wave channel experiment on natural seawater doped with  
603 Zobell growth medium, bacteria and phytoplankton (*Dunaliella tertiolecta*) cultures, Prather  
604 et al. (2013) also observed a link between heterotrophic bacteria and organic fraction while no  
605 correlation with chl-a was found, highlighting the necessity to study complex systems of all  
606 biological material (phytoplankton, prokaryotes, organic matter) for marine aerosol. Most  
607 likely, the observed differences between Prather et al. (2013) and this work have to do with  
608 the localized biogeochemical nature of the different experiments, causing variance in the  
609 chemical composition and organic fraction of the marine aerosol. An additional correlation  
610 ( $R^2=0.477$ ,  $p=1.2\times 10^{-5}$ ) exists with TEPs (Fig. 9E), a surface-active complex, variable mixture  
611 of organics (Filella, 2014; Passow, 2012). During BC, there is also a sigmoidal correlation  
612 between organic fraction and DOC concentrations ( $\chi^2=0.411$ ,  $p<0.00003$ ); data are  
613 unavailable for BV (Fig. 9F). Sigmoid fits are also shown in Figs. 8 and 9 for all biological  
614 parameters where they could be determined. Sigmoid fits might be more appropriate to use in  
615 many cases, to conceptually constrain the organic fraction of the primary marine aerosol to  
616 one regardless of the chl-a concentration. We have included both linear and sigmoid fits, with  
617 their respective  $R^2$  and  $\chi^2$  values for completeness.

618 We also wanted to see if correlations existed between different biogeochemical parameters  
619 and the temporal relative mode fractions shown in Fig. 2. Relative fractions of Modes 3 and 4  
620 (91.5 and 260nm, respectively) showed no clear correlations to any parameter. However,  
621 strong anti-correlations were observed between the Mode 1 (18.5nm) relative fraction and the  
622 abundances and concentrations of virus-like particles, heterotrophic prokaryotes and all

623 pigments previously discussed, except for alloxanthin, which had a positive correlation  
624 (correlations not shown). The relative fraction of Mode 2 (37.5nm) showed strong positive  
625 correlations with the abundances and concentrations of virus-like particles, heterotrophic  
626 prokaryotes, TEPs and all the pigments discussed, except for alloxanthin, where no  
627 correlation was observed (correlations not shown). This further supports the idea of an  
628 increase in the Mode 2 (Aitken mode) relative fraction during periods of high biological  
629 activity due to the higher concentrations of organic material, at the expense of Mode 1.

630 The control and acidified mesocosms showed no significant differences in terms of  
631 correlations between organic fraction and different biogeochemical parameters. For studies of  
632 marine aerosol, this indicates that any acidification effects on these biological parameters  
633 impacts the physical and chemical parameters of the aerosol much less than the natural  
634 variances caused by organic pre-bloom and bloom periods. It is not yet clear whether this  
635 observation can extend beyond the western Mediterranean Sea. However, it is important to  
636 note that due to the oligotrophic nature of the Mediterranean, even during the pre-bloom  
637 conditions at BV, the chl<sub>a</sub> concentrations and abundances of other parameters are still much  
638 lower than could occur in places like the North Atlantic Ocean.

#### 639 4. Conclusions

640 By performing marine aerosol bubble-bursting experiments over two large-scale campaigns,  
641 we were able to compare the effects of ocean acidification during pre-bloom and oligotrophic  
642 conditions on physical and chemical properties of Mediterranean Sea aerosol. It is important  
643 to note that there are additional effects, such as wind speed, precipitation levels, and  
644 temperatures, that could change with future climate change and that these were not included  
645 within this analysis; instead, we focused on ocean acidification effects on Mediterranean Sea  
646 plankton communities and subsequent effects on primary marine aerosol. Future studies will  
647 need to incorporate additional parameters to determine further effects on primary marine  
648 aerosol. Ocean acidification had no direct effect on the physical parameters (size distribution,  
649 mode diameter and number fraction) measured in either campaign, with similar trends seen  
650 for all three differently acidified mesocosms. Additionally, experiments including the  
651 enriched sea surface microlayer, which increased organic concentrations, showed no marked  
652 difference from the un-enriched mesocosm samples, indicating that enrichment did not  
653 influence the water uptake of the primary aerosol at the thermodynamic equilibrium reached  
654 in the CCN chamber.

655 Pre-bloom conditions at BV showed marked increases in the activation diameters and organic  
656 fractions (~64%) for all the mesocosms at SS=0.39% compared to non-bloom conditions at  
657 BC (~24%). At BV, larger particles (SS=0.08%) had smaller organic fractions (~38%). The  
658 organic fraction was strongly correlated with chl<sub>a</sub> and additional pigment concentrations, with  
659 weaker correlations observed for heterotrophic and autotrophic prokaryotes, virus-like  
660 particles, and *Synechococcus* abundances, and TEPs and DOC concentrations. Many of these  
661 correlations corresponded specifically with the increase in Mode 2 (the Aitken mode) and  
662 were anti-correlated with Mode 1 during the pre-bloom period. The CCN/CN<sub>average</sub> ratio also  
663 decreased during the pre-bloom period at BV as a probable consequence of the increased  
664 organic content during a pre-bloom period. The parameterization of the primary marine  
665 aerosol organic fraction as a function of chl<sub>a</sub> derived in the present work is a high estimate  
666 compared to the gathered parameterizations from the literature (with a higher organic fraction  
667 for a given chl<sub>a</sub> content), which may confirm that species other than chl<sub>a</sub>-rich species  
668 contribute to the organic content of marine aerosols in the Mediterranean atmosphere.

## 669 Author Contribution

670 K.S., F.G., C.G. designed the experiments and A.N.S., C.R., E.A., K.S. carried them out.  
671 Enriched microlayer data were provided by A.E. and W.L.; pigment data were provided by  
672 A.S. and F.G.; TEPs data were provided by S.M., M.-L.P., F.I., and S.A.; bacteria and virus  
673 data were provided by S.M., M.-L.P., A.T., and P.P; and DOC data were provided by J.L and  
674 C.G. A.N.S. and K.S. prepared the manuscript with contributions from all co-authors.

## 675 Acknowledgements

676 This work was supported by the MISTRALS/ChArMEX project and by the EC FP7 project  
677 'Mediterranean Sea Acidification in a changing climate' (MedSeA; grant agreement 265103).

678

## 679 References

- 680 Albert, M. F. M. A., Schaap, M., Manders, a. M. M., Scannell, C., O'Dowd, C. D., and de  
681 Leeuw, G.: Uncertainties in the determination of global sub-micron marine organic  
682 matter emissions, *Atmospheric Environment*, 57, 289-300, 2012.
- 683 Anttila, T., Vaattovaara, P., Komppula, M., Hyvärinen, A.-P., Lihavainen, H., Kerminen, V.-  
684 M., and Laaksonen, A.: Size-dependent activation of aerosols into cloud droplets at a  
685 subarctic background site during the second Pallas Cloud Experiment (2nd PaCE):  
686 method development and data evaluation, *Atmos. Chem. Phys.*, 9 (14), 4841-4854,  
687 doi:10.5194/acp-9-4841-2009, 2009.

- 688 Archer, S. D., Kimmance, S. A., Stephens, J. A., Hopkins, F. E., Bellerby, R. G. J., Schulz, K.  
689 G., Piontek, J., and Engel, a.: Contrasting responses of DMS and DMSP to ocean  
690 acidification in Arctic waters, *Biogeosciences*, 10 (3), 1893-1908, 2013.
- 691 Asa-Awuku, A., Engelhart, G. J., Lee, B. H., Pandis, S. N., and Nenes, A.: Relating CCN  
692 activity, volatility, and droplet growth kinetics of  $\beta$ -caryophyllene secondary organic  
693 aerosol, *Atmospheric Chemistry and Physics*, 9, 795-812, 2009.
- 694 Asmi, E., Freney, E., Hervo, M., Picard, D., Rose, C., Colomb, A., and Sellegri, K.: Aerosol  
695 cloud activation in summer and winter at puy-de-Dôme high altitude site in France,  
696 *Atmospheric Chemistry and Physics*, 12 (9), 23039-23091, 2012.
- 697 Ault, A. P., Moffet, R. C., Baltrusaitis, J., Collins, D. B., Ruppel, M. J., Cuadra-Rodriguez, L.  
698 A., Zhao, D., Guasco, T. L., Ebben, C. J., Geiger, F. M., Bertram, T. H., Prather, K.  
699 A., and Grassian, V. H.: Size-dependent changes in sea spray aerosol composition and  
700 properties with different seawater conditions, *Environmental Science & Technology*,  
701 47 (11), 5603-5612, 2013.
- 702 Barger, W. R. and Garrett, W. D.: Surface Active Organic Material in the Marine  
703 Atmosphere, *Journal of Geophysical Research*, 75 (24), 4561-4566, 1970.
- 704 Bates, T. S., Quinn, P. K., Frossard, A. A., Russell, L. M., Hakala, J., Petäjä, T., Kulmala, M.,  
705 Covert, D. S., Cappa, C. D., Li, S.-M., Hayden, K. L., Nuaaman, I., McLaren, R.,  
706 Massoli, P., Canagaratna, M. R., Onasch, T. B., Sueper, D., Worsnop, D. R., and  
707 Keene, W. C.: Measurements of ocean derived aerosol off the coast of California,  
708 *Journal of Geophysical Research*, 117 (D00V15), 2012.
- 709 Benner, R., Chemical composition and reactivity, in *Biogeochemistry of marine dissolved*  
710 *organic matter*, edited by D. A. Hansell and C. A. Carlson, pp. 59-90, Academic  
711 Press, San Diego, CA, 2002.
- 712 Bigg, E. K. and Leck, C.: The composition of fragments of bubbles bursting at the ocean  
713 surface, *Journal of Geophysical Research*, 113 (D11), D11209, 2008.
- 714 Blanchard, D. C.: Sea-to-Air Transport Surface Active Material, *Science*, 146 (13), 396-397,  
715 1964.
- 716 Blanchard, D. C. and Woodcock, A. H.: Bubble Formation and Modification in the Sea and its  
717 Meteorological Significance, *Tellus*, 9 (2), 145-158, 1957.
- 718 Callaghan, A. H., Deane, G. B., Stokes, M. D., and Ward, B.: Observed variation in the decay  
719 time of oceanic whitecap foam, *Journal of Geophysical Research: Oceans*, 117,  
720 C09015, 2012.
- 721 Cameron-Smith, P., Elliott, S., Maltrud, M., Erickson, D., and Wingenter, O.: Changes in  
722 dimethyl sulfide oceanic distribution due to climate change, *Geophysical Research*  
723 *Letters*, 38 (7), 2011.
- 724 Ciais, P., Sabine, C., Bala, G., Bopp, L., Brovkin, V., Canadell, J. G., Chhabra, A., DeFries, R.,  
725 Galloway, J., Heimann, M., Jones, C., Le Quéré, C., Myneni, R. B., Piao, S., and  
726 Thornton, P.: Carbon and Other Biogeochemical Cycles. In: *Climate Change 2013:*  
727 *The Physical Science Basis. Contribution of Working Group I to the Fifth Assessment*

- 728 Report of the Intergovernmental Panel on Climate Change, Stocker, B. D., Qin, D.,  
729 Plattner, G.-K., Tignor, M., Allen, S. K., Boschung, J., Nauels, A., Xia, Y., Bex, V.,  
730 and Midgley, P. M. 465-570. 2013. Cambridge, United Kingdom and New York, NY,  
731 USA, Cambridge University Press.
- 732 Clarke, A. D., Owens, S. R., and Zhou, J.: An ultrafine sea-salt flux from breaking waves:  
733 Implications for cloud condensation nuclei in the remote marine atmosphere, *Journal*  
734 *of Geophysical Research*, *111* (D6), D06202, 2006.
- 735 Collins, D. B., Ault, A. P., Moffet, R. C., Ruppel, M. J., Cuadra-Rodriguez, L. A., Guasco, T.  
736 L., Corrigan, C. E., Pedler, B. E., Azam, F., Aluwihare, L. I., Bertram, T. H., Roberts,  
737 G. C., Grassian, V. H., and Prather, K. A.: Impact of marine biogeochemistry on the  
738 chemical mixing state and cloud forming ability of nascent sea spray aerosol, *Journal*  
739 *of Geophysical Research: Atmospheres*, *118* (15), 8553-8565, 2013.
- 740 Cunliffe, M., Engel, A., Frka, S., Gasparovic, B., Guitart, C., Murrell, J. C., Salter, M., Stolle,  
741 C., Upstill-Goddard, R., and Wurl, O.: Sea surface microlayers: A unified  
742 physicochemical and biological perspective of the air–ocean interface, *Progress in*  
743 *Oceanography*, *109*, 104-116, 2013.
- 744 D'Ortenzio, F. and Ribera d'Alcalà, M.: On the trophic regimes of the Mediterranean Sea: a  
745 satellite analysis, *Biogeosciences*, *6*, 139-148, 2009.
- 746 Doney, S. C., Ruckelshaus, M., Duffy, J. E., Barry, J. P., Chan, F., English, C. A., Galindo, H.  
747 M., Grebmeier, J. M., Hollowed, A. B., Knowlton, N., Polovina, J., Rabalais, N. N.,  
748 Sydeman, W. J., and Talley, L. D.: Climate Change Impacts on Marine Ecosystems,  
749 *Annual review of marine science*, *4* ( 11-37, doi: 10.1146/annurev-marine-041911-  
750 111611, 2012.
- 751 Ducklow, H. W., Carlson, C. A., Bates, N. R., Knap, A. H., Michaels, A. F., Jickells, T., Le,  
752 P. J., Williams, B., and McCave, I. N.: Dissolved Organic Carbon as a Component of  
753 the Biological Pump in the North Atlantic Ocean, *Philosophical Transactions of The*  
754 *Royal Society B*, *348* (1324), 161-167, 1995.
- 755 Engel, A., Determination of marine gel particles, in *Practical Guidelines for the Analysis of*  
756 *Seawater*, edited by O. Wurl, pp. 125-142, CRC Press, Boca Raton, Florida, 2009.
- 757 Facchini, M. C., Rinaldi, M., Decesari, S., Carbone, C., Finessi, E., Mircea, M., Fuzzi, S.,  
758 Ceburnis, D., Flanagan, R., Nilsson, E. D., de Leeuw, G., Martino, M., Woeltjen, J.,  
759 and O'Dowd, C. D.: Primary submicron marine aerosol dominated by insoluble  
760 organic colloids and aggregates, *Geophysical Research Letters*, *35* (17), L17814,  
761 2008.
- 762 Filella, M.: Understanding what we are measuring: standards and quantification of natural  
763 organic matter, *Water research*, *50*, 287-293, 2014.
- 764 Fuentes, E., Coe, H., Green, D., de Leeuw, G., and McFiggans, G.: Laboratory-generated  
765 primary marine aerosol via bubble-bursting and atomization, *Atmospheric*  
766 *Measurement Techniques*, *3* (1), 141-162, 2010a.
- 767 Fuentes, E., Coe, H., Green, D., de Leeuw, G., and McFiggans, G.: On the impacts of  
768 phytoplankton-derived organic matter on the properties of the primary marine aerosol

- 769 – Part 1: Source fluxes, *Atmospheric Chemistry and Physics*, 10 (19), 9295-9317,  
770 2010b.
- 771 Fuentes, E., Coe, H., Green, D., and McFiggans, G.: On the impacts of phytoplankton-derived  
772 organic matter on the properties of the primary marine aerosol – Part 2: Composition,  
773 hygroscopicity and cloud condensation activity, *Atmospheric Chemistry and Physics*,  
774 11 (6), 2585-2602, 2011.
- 775 Galgani, L., Stolle, C., Endres, S., Schulz, K. G., and Engel, A.: Effects of ocean acidification  
776 on the biogenic composition of the sea-surface microlayer: Results from a mesocosm  
777 study, *Journal of Geophysical Research: Oceans*, 119 (11), 7911-7924, DOI:  
778 10.1002/2014JC010188, 2014.
- 779 Gantt, B. and Meskhidze, N.: The physical and chemical characteristics of marine primary  
780 organic aerosol: a review, *Atmospheric Chemistry and Physics*, 13 (8), 3979-3996,  
781 2013.
- 782 Gantt, B., Meskhidze, N., Facchini, M. C., Rinaldi, M., Ceburnis, D., and O'Dowd, C. D.:  
783 Wind speed dependent size-resolved parameterization for the organic mass fraction of  
784 sea spray aerosol, *Atmospheric Chemistry and Physics*, 11 (16), 8777-8790, 2011.
- 785 Garrett, W. D.: The organic chemical composition of the ocean surface, *Deep Sea Research*  
786 *and Oceanographic Abstracts*, 14 (2), 221-227, 1967.
- 787 Gazeau, F., Ziveri, P., Sallon, A., Lejeune, P., Gobert, S., Maugeudre, L., Louis, J., Alliouane,  
788 S., Taillandier, V., Louis, F., Obolensky, G., Grisoni, J.-M., Delissanti, W., Luquet,  
789 D., Robin, D., Hesse, B., and Guieu, C.: First mesocosm experiments to study the  
790 impacts of ocean acidification on the plankton communities in the NW Mediterranean  
791 Sea (MedSeA project), *submitted*.
- 792 Gruber, D. F., Simjouw, J.-P., Seitzinger, S. P., and Taghon, G. L.: Dynamics and  
793 characterization of refractory dissolved organic matter produced by a pure bacterial  
794 culture in an experimental predator-prey system, *Applied and environmental*  
795 *microbiology*, 72 (6), 4184-4191, 2006.
- 796 Grythe, H., Ström, J., Krejci, R., Quinn, P., and Stohl, a.: A review of sea-spray aerosol  
797 source functions using a large global set of sea salt aerosol concentration  
798 measurements, *Atmospheric Chemistry and Physics*, 14 (3), 1277-1297, 2014.
- 799 Guieu, C., Dulac, F., Ridame, C., and Pondaven, P.: Introduction to project DUNE, a DUst  
800 experiment in a low Nutrient, low chlorophyll Ecosystem, *Biogeosciences*, 11 (2),  
801 425-442, 2014.
- 802 Hansell, D. A., Carlson, C. A., Repeta, D. J., and Schlitzer, R.: Dissolved Organic Matter in  
803 the Ocean, *Oceanography*, 22 (4), 202-211, 2009.
- 804 Hare, C. E., Leblanc, K., DiTullio, G. R., Kudela, R. M., Zhang, Y., Lee, P. A., Riseman, S.,  
805 and Hutchins, D. A.: Consequences of increased temperature and CO<sub>2</sub> for  
806 phytoplankton community structure in the Bering Sea, *Marine Ecology Progress*  
807 *Series*, 352, 9-16, 2007.

- 808 Hegg, D. A., Covert, D. S., Jonsson, H. H., and Woods, R.: Differentiating natural and  
 809 anthropogenic cloud condensation nuclei in the California coastal zone, *Tellus B*, 61  
 810 (4), 2009.
- 811 Hultin, K., Krejci, R., Pinhassi, J., Gomez-Consarnau, L., Mårtensson, E. M., Hagström, Å.,  
 812 and Nilsson, E. D.: Aerosol and bacterial emissions from Baltic Seawater,  
 813 *Atmospheric Research*, 99 (1), 1-14, 2011.
- 814 Hultin, K., Nilsson, E. D., Krejci, R., Mårtensson, E. M., Ehn, M., Hagström, Å., and de  
 815 Leeuw, G.: In situ laboratory sea spray production during the Marine Aerosol  
 816 Production 2006 cruise on the northeastern Atlantic Ocean, *Journal of Geophysical*  
 817 *Research*, 115 (D6), D06201, 2010.
- 818 IPCC: Climate Change 2013: The Physical Science Basis. Contribution of Working Group I  
 819 to the Fifth Assessment Report of the Intergovernmental Panel on Climate Change,  
 820 Stocker, T. F., Qin, D., Plattner, G.-K., Tignor, M., Allen, S. K., Boschung, J., Nauels,  
 821 A., Xia, Y., Bex, V., and Midgley, P. M. 2013. Cambridge, United Kingdom and New  
 822 York, NY, USA, Cambridge University Press.
- 823 Irwin, A. J. and Oliver, M. J.: Are ocean deserts getting larger?, *Geophysical Research*  
 824 *Letters*, 36 (18), L18609, 2009.
- 825 Jiao, N., Herndl, G. J., Hansell, D. A., Benner, R., Kattner, G., Wilhelm, S. W., Kirchman, D.  
 826 L., Weinbauer, M. G., Luo, T., Chen, F., and Azam, F.: Microbial production of  
 827 recalcitrant dissolved organic matter: long-term carbon storage in the global ocean,  
 828 *Nature reviews. Microbiology*, 8 (8), 593-599, 2010.
- 829 Keene, W. C., Maring, H., Maben, J. R., Kieber, D. J., Pszenny, A. A. P., Dahl, E. E.,  
 830 Izaguirre, M. A., Davis, A. J., Long, M. S., Zhou, X., Smoydzin, L., and Sander, R.:  
 831 Chemical and physical characteristics of nascent aerosols produced by bursting  
 832 bubbles at a model air-sea interface, *Journal of Geophysical Research*, 112 (D21),  
 833 D21202, 2007.
- 834 King, S. M., Butcher, A. C., Rosenoern, T., Coz, E., Lieke, K. I., de Leeuw, G., Nilsson, E.  
 835 D., and Bilde, M.: Investigating Primary Marine Aerosol Properties: CCN Activity of  
 836 Sea Salt and Mixed Inorganic-Organic Particles, *Environmental Science &*  
 837 *Technology*, 2012.
- 838 Langmann, B., Scannell, C., and O'Dowd, C.: New Directions: Organic matter contribution to  
 839 marine aerosols and cloud condensation nuclei, *Atmospheric Environment*, 42 (33),  
 840 7821-7822, 2008.
- 841 Le Quéré, C., Moriarty, R., Andrew, R. M., Peters, G. P., Ciais, P., Friedlingstein, P., Jones,  
 842 S. D., Sitch, S., Tans, P., Arneeth, A., Boden, T. A., Bopp, L., Bozec, Y., Canadell, J.  
 843 G., Chevallier, F., Cosca, C. E., Harris, I., Hoppema, M., Houghton, R. A., House, J.  
 844 I., Jain, A., Johannessen, T., Kato, E., Keeling, R. F., Kitidis, V., Klein Goldewijk, K.,  
 845 Koven, C., Landa, C. S., Landschützer, P., Lenton, A., Lima, I. D., Marland, G.,  
 846 Mathis, J. T., Metzl, N., Nojiri, Y., Olsen, A., Ono, T., Peters, W., Pfeil, B., Poulter,  
 847 B., Raupach, M. R., Regnier, P., Rödenbeck, C., Saito, S., Salisbury, J. E., Schuster,  
 848 U., Schwinger, J., Séférian, R., Segschneider, J., Steinhoff, T., Stocker, B. D., Sutton,  
 849 A. J., Takahashi, T., Tilbrook, B., van der Werf, G. R., Viovy, N., Wang, Y.-P.,

- 850 Wanninkhof, R., Wiltshire, A., and Zeng, N.: Global carbon budget 2014, *Earth Syst.*  
851 *Sci. Data Discuss.*, 7 (2), 521-610, 2014.
- 852 Lewis, S. and Schwartz, R.: Sea salt aerosol production: mechanisms, methods, measurements,  
853 and models - a critical review, 2004. Washington, DC.
- 854 Lion, L. W. and Leckie, J. O.: The Biogeochemistry of the air-sea interface, *Annual Review of*  
855 *Earth and Planetary Sciences*, 9, 449-486, 1981.
- 856 Long, M. S., Keene, W. C., Kieber, D. J., Erickson, D. J., and Maring, H.: A sea-state based  
857 source function for size- and composition-resolved marine aerosol production,  
858 *Atmospheric Chemistry and Physics*, 11, 1203-1216, 2011.
- 859 Mårtensson, E. M., Nilsson, E. D., de Leeuw, G., Cohen, L. H., and Hansson, H.-C.:  
860 Laboratory simulations and parameterization of the primary marine aerosol  
861 production, *Journal of Geophysical Research*, 108 (D9), 4297, 2003.
- 862 Matrai, P. A., Tranvik, L., Leck, C., and Knulst, J. C.: Are high Arctic surface microlayers a  
863 potential source of aerosol organic precursors?, *Marine Chemistry*, 108 (1-2), 109-122,  
864 2008.
- 865 Moore, M. J. K., Furutani, H., Roberts, G. C., Moffet, R. C., Gilles, M. K., Palenik, B., and  
866 Prather, K. A.: Effect of organic compounds on cloud condensation nuclei (CCN)  
867 activity of sea spray aerosol produced by bubble bursting, *Atmospheric Environment*,  
868 45 (39), 7462-7469, 2011.
- 869 Moutin, T. and Raimbault, P.: Primary production, carbon export and nutrients availability in  
870 western and eastern Mediterranean Sea in early summer 1996 (MINOS cruise),  
871 *Journal of Marine Systems*, 33-34, 273-288, 2002.
- 872 Murphy, D. M., Anderson, J. R., Quinn, P. K., McInnes, L. M., Brechtel, F. J., Kreidenweis,  
873 S. M., Middlebrook, A. M., Pósfai, M., Thomson, D. S., and Buseck, P. R.: Influence  
874 of sea-salt on aerosol radiative properties in the Southern Ocean marine boundary  
875 layer, *Nature*, 392 (1994), 62-65, 1998.
- 876 Novakov, T. and Corrigan, C. E.: Cloud condensation nucleus activity of the organic  
877 component of biomass smoke particles, *Geophysical Research Letters*, 23 (16), 2141-  
878 2144, DOI: 10.1029/96GL01971, 1996.
- 879 Novakov, T. and Penner, J. E.: Large contribution of organic aerosols to cloud-condensation-  
880 nuclei concentrations, *Nature*, 365, 823-826, doi:10.1038/365823a0, 1993.
- 881 O'Dowd, C. D., Facchini, M. C., Cavalli, F., Ceburnis, D., Mircea, M., Decesari, S., Fuzzi, S.,  
882 Yoon, Y. J., and Putaud, J.-P.: Biogenically driven organic contribution to marine  
883 aerosol, *Nature*, 431 (October), 676-680, 2004.
- 884 O'Dowd, C. D., Langmann, B., Varghese, S., Scannell, C., Ceburnis, D., and Facchini, M. C.:  
885 A combined organic-inorganic sea-spray source function, *Geophysical Research*  
886 *Letters*, 35 (1), L01801, 2008.

- 887 Ogawa, H., Amagai, Y., Koike, I., Kaiser, K., and Benner, R.: Production of refractory  
888 dissolved organic matter by bacteria, *Science (New York, N. Y. )*, 292 (5518), 917-920,  
889 2001.
- 890 Passow, U.: The abiotic formation of TEP under different ocean acidification scenarios,  
891 *Marine Chemistry*, 128-129 , 72-80, 2012.
- 892 Petters, M. D. and Kreidenweis, S. M.: A single parameter representation of hygroscopic  
893 growth and cloud condensation nucleus activity, *Atmospheric Chemistry and Physics*,  
894 7 (8), 1961-1971, 2007.
- 895 Polovina, J. J., Howell, E. A., and Abecassis, M.: Ocean's least productive waters are  
896 expanding, *Geophysical Research Letters*, 35 (3), L03618, 2008.
- 897 Prather, K. A., Bertram, T. H., Grassian, V. H., Deane, G. B., Stokes, M. D., Demott, P. J.,  
898 Aluwihare, L. I., Palenik, B. P., Azam, F., Seinfeld, J. H., Moffet, R. C., Molina, M. J.,  
899 Cappa, C. D., Geiger, F. M., Roberts, G. C., Russell, L. M., Ault, A. P., Baltrusaitis, J.,  
900 Collins, D. B., Corrigan, C. E., Cuadra-Rodriguez, L. A., Ebben, C. J., Forestieri, S.  
901 D., Guasco, T. L., Hersey, S. P., Kim, M. J., Lambert, W. F., Modini, R. L., Mui, W.,  
902 Pedler, B. E., Ruppel, M. J., Ryder, O. S., Schoepp, N. G., Sullivan, R. C., and Zhao,  
903 D.: Bringing the ocean into the laboratory to probe the chemical complexity of sea  
904 spray aerosol, *Proceedings of the National Academy of Sciences of the United States of*  
905 *America*, 110 (19), 7550-7555, 2013.
- 906 Pringle, K. J., Tost, H., Pozzer, a., Pöschl, U., and Lelieveld, J.: Global distribution of the  
907 effective aerosol hygroscopicity parameter for CCN activation, *Atmospheric*  
908 *Chemistry and Physics*, 10 (12), 5241-5255, 2010.
- 909 Quinn, P. K. and Bates, T. S.: The case against climate regulation via oceanic phytoplankton  
910 sulphur emissions, *Nature*, 480 (7375), 51-56, 2011.
- 911 Riebesell, U., Bellerby, R. G. J., Grossart, H.-P., and Thingstad, F.: Mesocosm CO<sub>2</sub>  
912 perturbation studies: from organism to community level, *Biogeosciences*, 5 (4), 1157-  
913 1164, 2008.
- 914 Riebesell, U., Czerny, J., von Bröckel, K., Boxhammer, T., Büdenbender, J., Deckelnick, M.,  
915 Fischer, M., Hoffmann, D., Krug, S. A., Lentz, U., Ludwig, A., Mucche, R., and  
916 Schulz, K. G.: Technical Note: A mobile sea-going mesocosm system – new  
917 opportunities for ocean change research, *Biogeosciences*, 10 (3), 1835-1847, 2013.
- 918 Riebesell, U. and P. D. Tortell, Effects of ocean acidification on pelagic organisms and  
919 ecosystems., in *Ocean Acidification*, edited by J. P. Gattuso and L. Hansson, Oxford  
920 University Press, Oxford, 2011.
- 921 Rinaldi, M., Fuzzi, S., Decesari, S., Marullo, S., Santoleri, R., Provenzale, A., von  
922 Hardenberg, J., Ceburnis, D., Vaishya, A., O'Dowd, C. D., and Facchini, M. C.: Is  
923 chlorophyll-a the best surrogate for organic matter enrichment in submicron primary  
924 marine aerosol?, *Journal of Geophysical Research: Atmospheres*, 118 (10), 4964-  
925 4973, 2013.

- 926 Roberts, G. C. and Nenes, A.: A Continuous-Flow Streamwise Thermal-Gradient CCN  
927 Chamber for Atmospheric Measurements, *Aerosol Science and Technology*, 39 (3),  
928 206-221, 2005.
- 929 Russell, L. M., Hawkins, L. N., Frossard, A., Quinn, P. K., and Bates, T. S.: Carbohydrate-  
930 like composition of submicron atmospheric particles and their production from ocean  
931 bubble bursting, *Proceedings of the National Academy of Sciences of the United States*  
932 *of America*, 107 (15), 6652-6657, 2010.
- 933 Schulz, K. G., Bellerby, R. G. J., Brussaard, C. P. D., Büdenbender, J., Czerny, J., Engel, a.,  
934 Fischer, M., Koch-Klavsen, S., Krug, S. A., Lischka, S., Ludwig, A., Meyerhöfer, M.,  
935 Nondal, G., Silyakova, A., Stuhr, A., and Riebesell, U.: Temporal biomass dynamics  
936 of an Arctic plankton bloom in response to increasing levels of atmospheric carbon  
937 dioxide, *Biogeosciences*, 10 (1), 161-180, doi:10.5194/bg-10-161-2013, 2013.
- 938 Sciare, J., Favez, O., Sarda-Estève, R., Oikonomou, K., Cachier, H., and Kazan, V.: Long-  
939 term observations of carbonaceous aerosols in the Austral Ocean atmosphere:  
940 Evidence of a biogenic marine organic source, *Journal of Geophysical Research*, 114  
941 (D15), D15302, 2009.
- 942 Sciare, J., Mihalopoulos, N., and Dentener, F. J.: Interannual variability of atmospheric  
943 dimethylsulfide in the southern Indian Ocean, *Journal of Geophysical Research*, 105  
944 (D21), 26369, 2000.
- 945 Sellegri, K., O'Dowd, C. D., Yoon, Y. J., Jennings, S. G., and de Leeuw, G.: Surfactants and  
946 submicron sea spray generation, *Journal of Geophysical Research*, 111 (D22),  
947 D22215, 2006.
- 948 Siokou-Frangou, I., Christaki, U., Mazzocchi, M. G., Montresor, M., Ribera d'Alcalà, M.,  
949 Vaqué, D., and Zingone, a.: Plankton in the open Mediterranean Sea: a review,  
950 *Biogeosciences*, 7 (5), 1543-1586, 2010.
- 951 Spracklen, D. V., Arnold, S. R., Sciare, J., Carslaw, K. S., and Pio, C.: Globally significant  
952 oceanic source of organic carbon aerosol, *Geophysical Research Letters*, 35 (12),  
953 L12811, 2008.
- 954 Stewart, R. I. A., M. Dossena, D. A. Bohan, E. Jeppesen, R. L. Kordas, M. E. Ledger, M.  
955 Meerhoff, B. Moss, C. Mulder, J. B. Shurin, B. Suttle, R. Thompson, M. Trimmer, and  
956 G. Woodward, Mesocosm Experiments as a Tool for Ecological Climate-Change  
957 Research. In: Global Change in Multispecies Systems, Part 3., in *Advances in*  
958 *Ecological research*, edited by G. Woodward and E. J. O'Gorman, pp. 71-181,  
959 Elsevier, 2013.
- 960 Stommel, Y. G. and Riebel, U.: A new corona discharge-based aerosol charger for submicron  
961 particles with low initial charge, *Journal of Aerosol Science*, 35 (9), 1051-1069, 2004.
- 962 Stommel, Y. G. and Riebel, U.: A corona-discharge-based aerosol neutralizer designed for use  
963 with the SMPS-system, *Journal of Electrostatics*, 63 (6-10), 917-921, 2005.
- 964 The Mermex Group: Marine ecosystems responses to climatic and anthropogenic forcings in  
965 the Mediterranean, *Progress in Oceanography*, 91 (2), 97-166, 2011.

- 966 Tyree, C. A., Hellion, V. M., Alexandrova, O. A., and Allen, J. O.: Foam droplets generated  
967 from natural and artificial seawaters, *Journal of Geophysical Research*, 112 (D12),  
968 D12204, 2007.
- 969 Vignati, E., Facchini, M. C., Rinaldi, M., Scannell, C., Ceburnis, D., Sciare, J., Kanakidou,  
970 M., Myriokefalitakis, S., Dentener, F., and O'Dowd, C. D.: Global scale emission and  
971 distribution of sea-spray aerosol: Sea-salt and organic enrichment, *Atmospheric*  
972 *Environment*, 44 (5), 670-677, 2010.
- 973 Weinbauer, M. G., X. Mari, and J.-P. Gattuso, Effect of Ocean Acidification on the Diversity  
974 and Activity of Heterotrophic Marine Microorganisms, in *Ocean Acidification*, edited  
975 by J.-P. Gattuso and L. Hansson, Oxford University Press, Oxford, 2011.
- 976 Woodhouse, M. T., Mann, G. W., Carslaw, K. S., and Boucher, O.: Sensitivity of cloud  
977 condensation nuclei to regional changes in dimethyl-sulphide emissions, *Atmospheric*  
978 *Chemistry and Physics*, 13 (5), 2723-2733, 2013.
- 979 Yoon, Y. J., Ceburnis, D., Cavalli, F., Jourdan, O., Putaud, J. P., Facchini, M. C., Decesari, S.,  
980 Fuzzi, S., Sellegri, K., Jennings, S. G., and O'Dowd, C. D.: Seasonal characteristics of  
981 the physicochemical properties of North Atlantic marine atmospheric aerosols,  
982 *Journal of Geophysical Research*, 112 (D04206), 2007.
- 983 Zábory, J., Krejci, R., Ekman, a. M. L., Mårtensson, E. M., Ström, J., de Leeuw, G., and  
984 Nilsson, E. D.: Wintertime Arctic Ocean sea water properties and primary marine  
985 aerosol concentrations, *Atmospheric Chemistry and Physics*, 12 (21), 10405-10421,  
986 2012a.
- 987 Zábory, J., Matisans, M., Krejci, R., Nilsson, E. D., and Ström, J.: Artificial primary marine  
988 aerosol production: a laboratory study with varying water temperature, salinity, and  
989 succinic acid concentration, *Atmospheric Chemistry and Physics*, 12 (22), 10709-  
990 10724, 2012b.
- 991  
992  
993  
994  
995  
996  
997  
998  
999  
1000  
1001  
1002  
1003  
1004  
1005  
1006  
1007  
1008  
1009  
1010

1011 Table 1. Calibration information at varying temperature gradients for NaCl (35g/L) in tank

Temperature Gradient	Activation Diameter (nm)	Supersaturation, SS (%)
dT6	42.497±1.82	0.39
dT3	122.915±8.65	0.08

1012

1013

1014 Table 2. Modal diameter (nm) and number fraction averages from the size distributions for  
1015 both campaigns, including data from both supersaturations and microlayer enriched  
1016 experiments. Lognormal modal diameters and number fractions from Fuentes et al. (2010a)  
1017 are also shown.

	BC (SS=0.39% and enriched)		BV (SS=0.39%+0.08% and enriched)		Artificial Sea Water Fuentes et al., (2010)	
	Diameter	Fraction	Diameter	Fraction	Diameter	Fraction
Mode 1	17 ± 1.2	0.32	20 ± 0.07	0.19	14	0.38
Mode 2	38 ± 1.3	0.30	37 ± 2.5	0.48	48	0.32
Mode 3	91 ± 2.1	0.27	92 ± 3.4	0.24	124	0.17
Mode 4	260 ± 2.0	0.11	260 ± 6.0	0.09	334	0.13

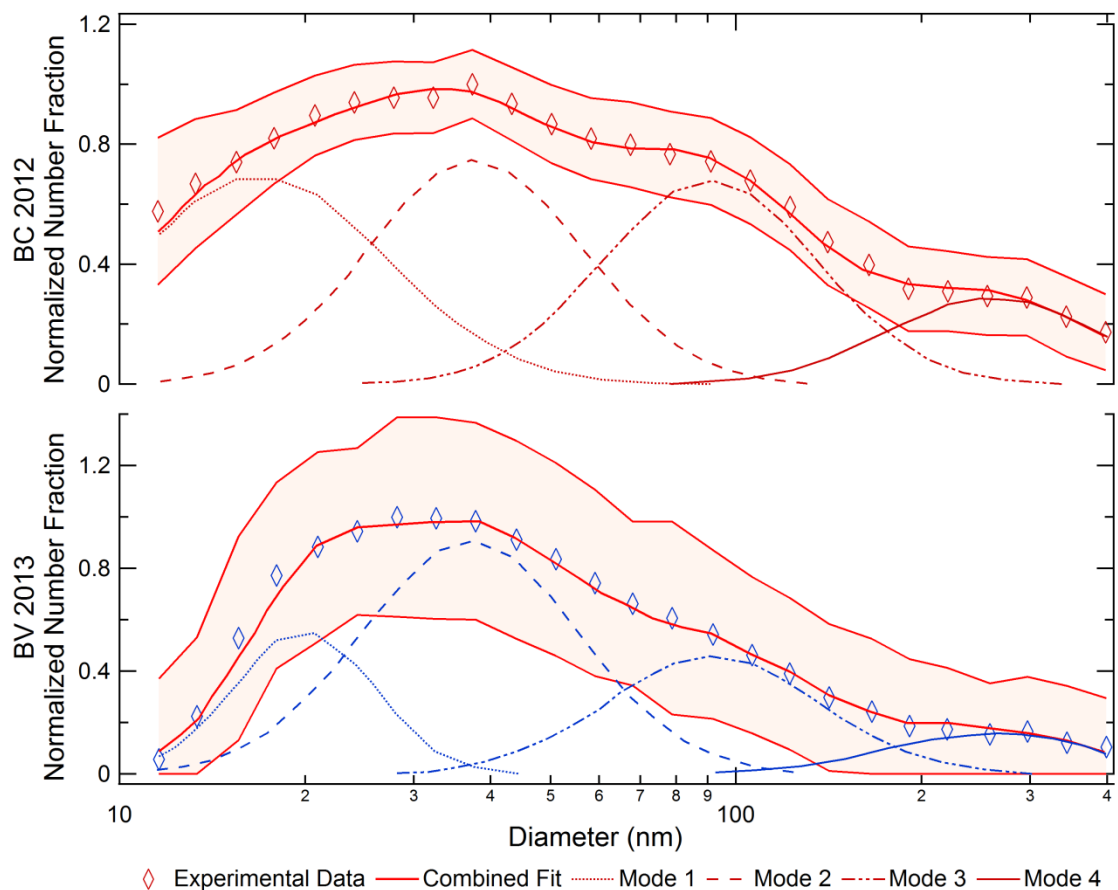
1018

1019

1020 Table 3. Average activation diameters, kappa values and organic fractions for both campaigns  
1021 and supersaturations.

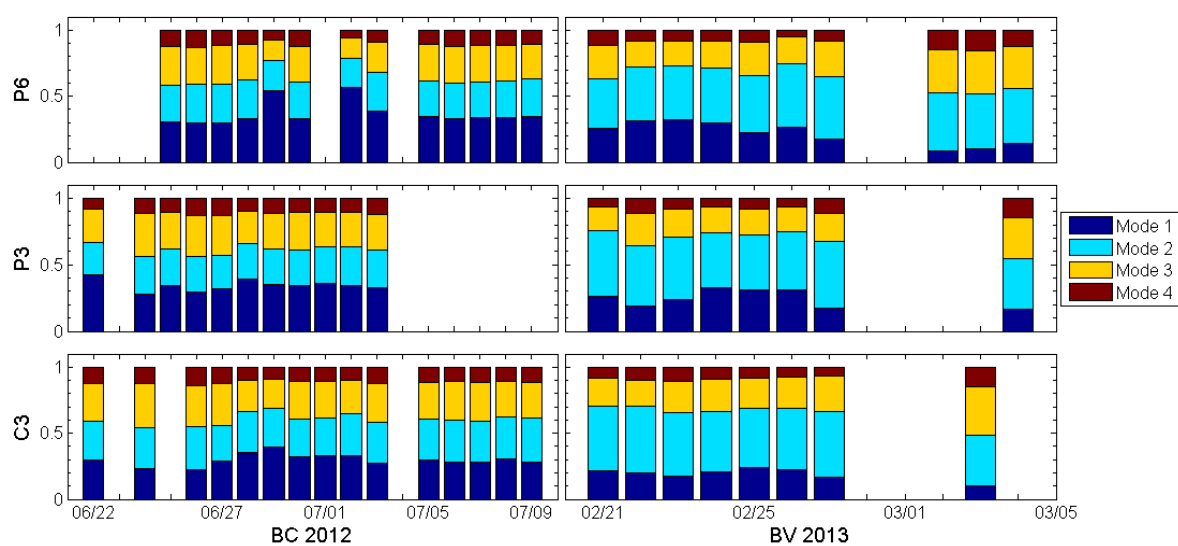
	Mesocosm	Activation Diameter (nm)	$\kappa$	Organic Fraction	
BC	SS = 0.39%	C3	47.5 ± 1.6	0.88 ± 0.11	0.29 ± 0.09
		C3, enriched	46.8 ± 4.1	0.92 ± 0.08	0.26 ± 0.07
		P3	45.8 ± 1.8	1.00 ± 0.19	0.20 ± 0.16
		P3, enriched	48.9 ± 6.1	0.81 ± 0	0.35 ± 0
		P6	45.7 ± 1.6	1.00 ± 0.23	0.20 ± 0.18
		P6, enriched	46.7 ± 3.4	0.93 ± 0.08	0.26 ± 0.06
BV	SS=0.39%	C3	61.8 ± 2.2	0.40 ± 0.09	0.68 ± 0.07
		C3, enriched	51.9 ± 4.8	0.68 ± 0	0.46 ± 0
		P3	61.2 ± 2.1	0.41 ± 0.12	0.67 ± 0.10
		P6	59.1 ± 1.9	0.47 ± 0.15	0.63 ± 0.12
		P6, enriched	53.9 ± 3.6	0.61 ± 0.10	0.52 ± 0.08
		Outside	54.2 ± 3.6	0.59 ± 0.14	0.53 ± 0.11
		Outside, enriched	55.5 ± 3.0	0.55 ± 0.07	0.56 ± 0.05
	SS=0.08%	C3	146.0 ± 16.6	0.72 ± 0.14	0.43 ± 0.12
		C3, enriched	148.5 ± 37.1	0.69 ± 0	0.45 ± 0
		P6	137.1 ± 15.5	0.87 ± 0.13	0.31 ± 0.11

1022



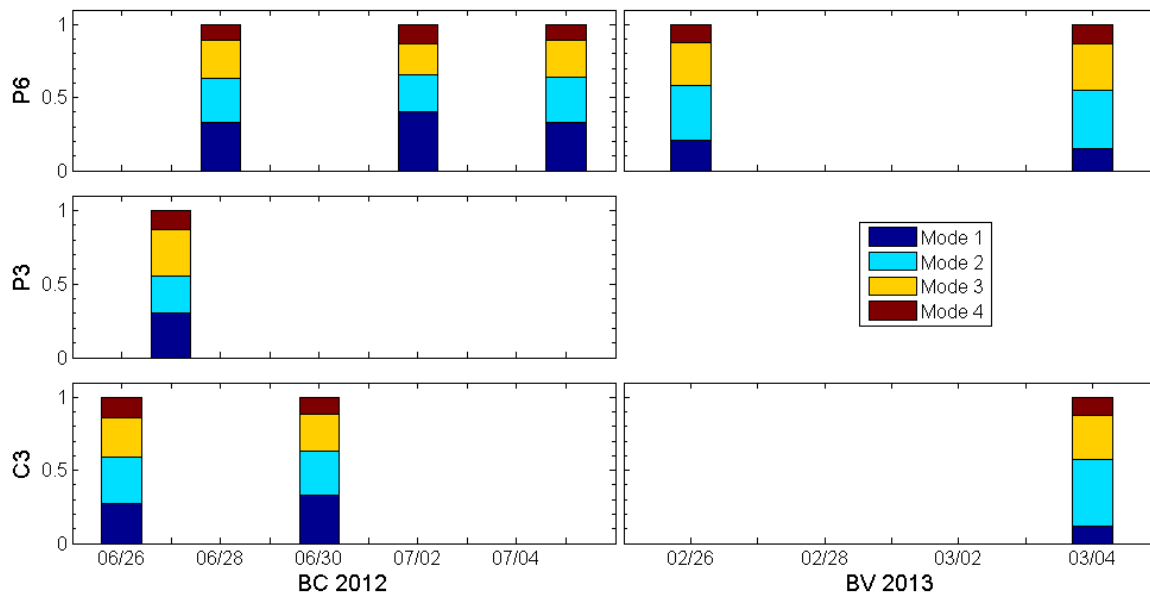
1023

1024 Figure 1. Average size distributions for each campaign (Bay of Calvi, BC, and Bay of  
 1025 Villefranche, BV) fit with 4 lognormal modes. Each campaign average is taken from the  
 1026 supersaturations (SS=0.08% & 0.39%) used for all three mesocosms and includes all enriched  
 1027 samples as well.

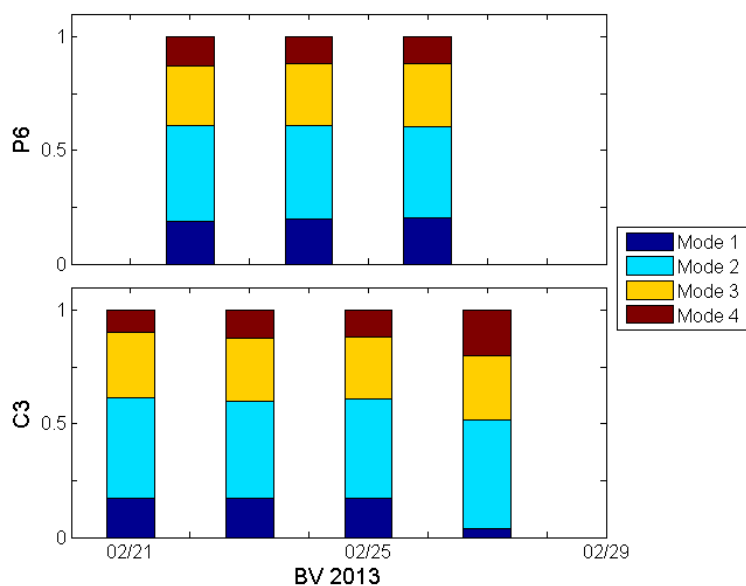


1028

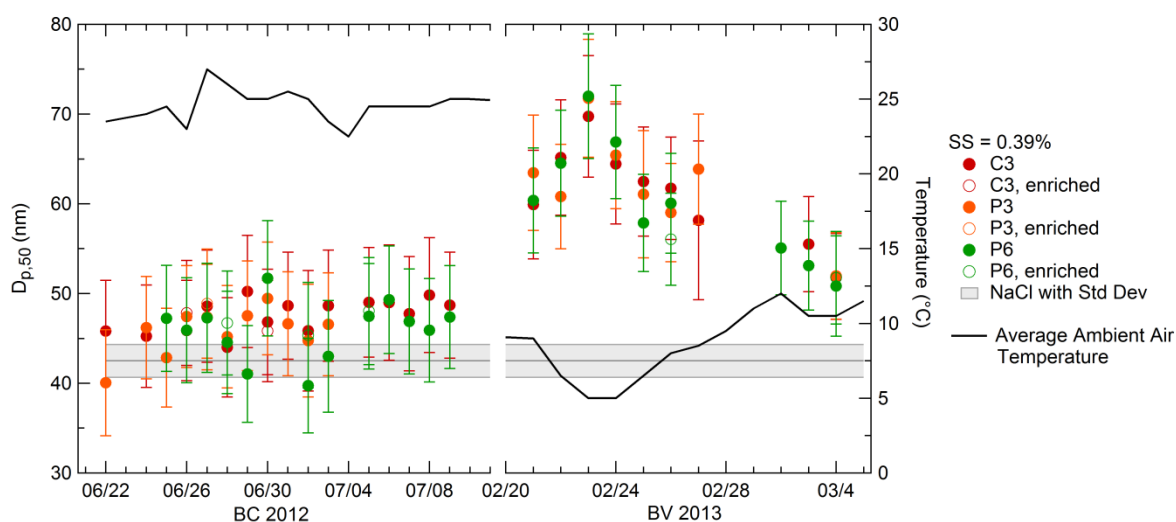
1029 Figure 2. Number fraction of DMPS lognormal modes from all mesocosms (SS=0.39%) at BC  
 1030 and BV.



1031  
 1032 Figure 3. Number fraction of DMPS lognormal modes from microlayer enriched samples  
 1033 (SS=0.39%) at BC and BV.

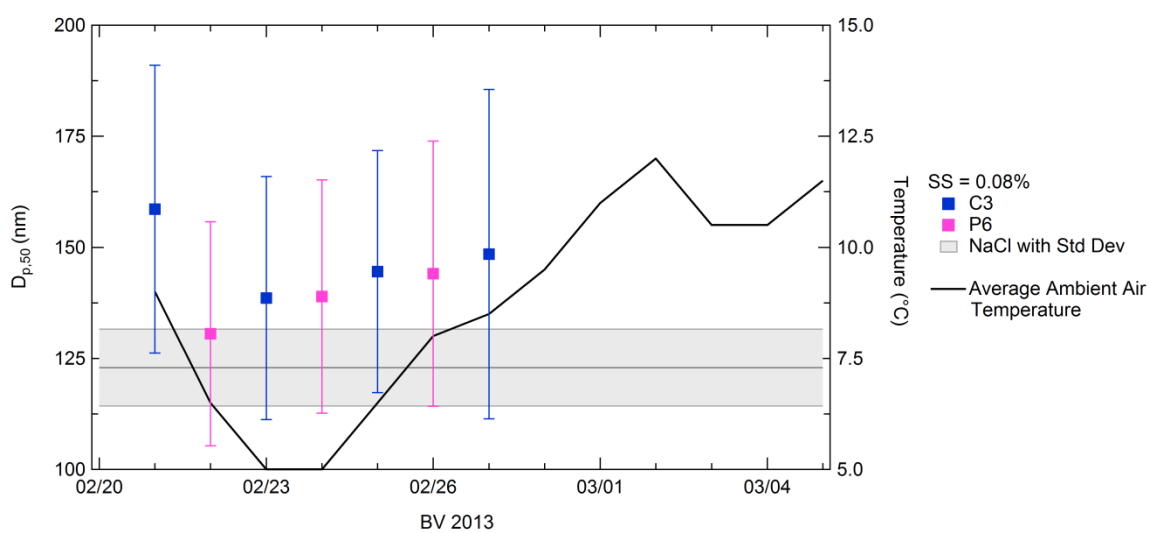


1034  
 1035 Figure 4. Number fraction of DMPS lognormal modes tested at SS=0.08% for mesocosms C3  
 1036 and P6 at BV.



1037

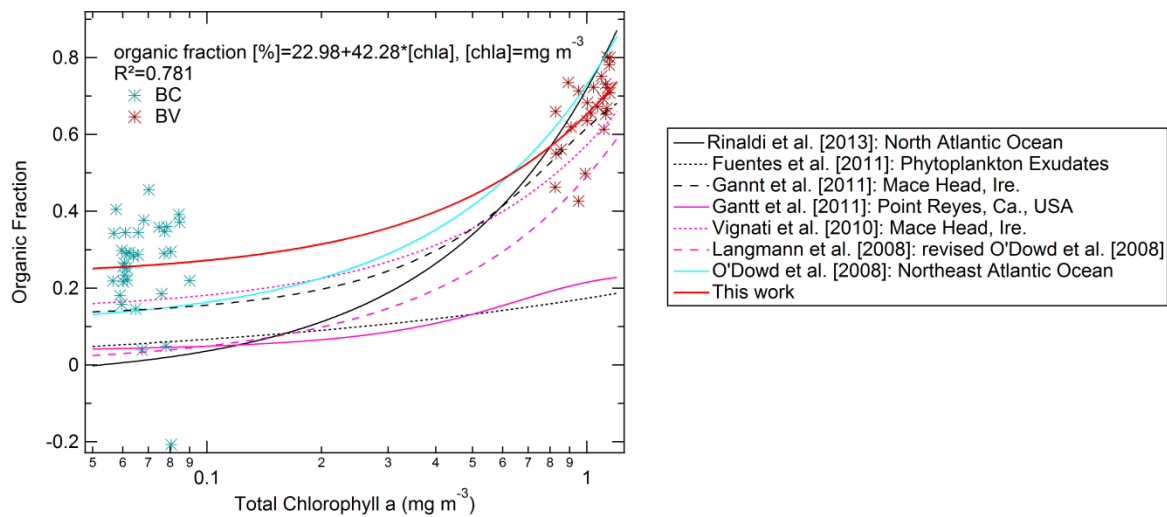
1038 Figure 5. Activation diameter and ambient air temperatures for BC and BV. Data is shown for  
 1039 SS=0.39% (dT6), including the microlayer enriched experiments. The shaded bar indicates the  
 1040 NaCl activation diameter at the given supersaturation.



1041

1042 Figure 6. Activation diameter and ambient air temperatures for BV. Data is shown for  
 1043 SS=0.08% (dT3). The shaded bar indicates the NaCl activation diameter.

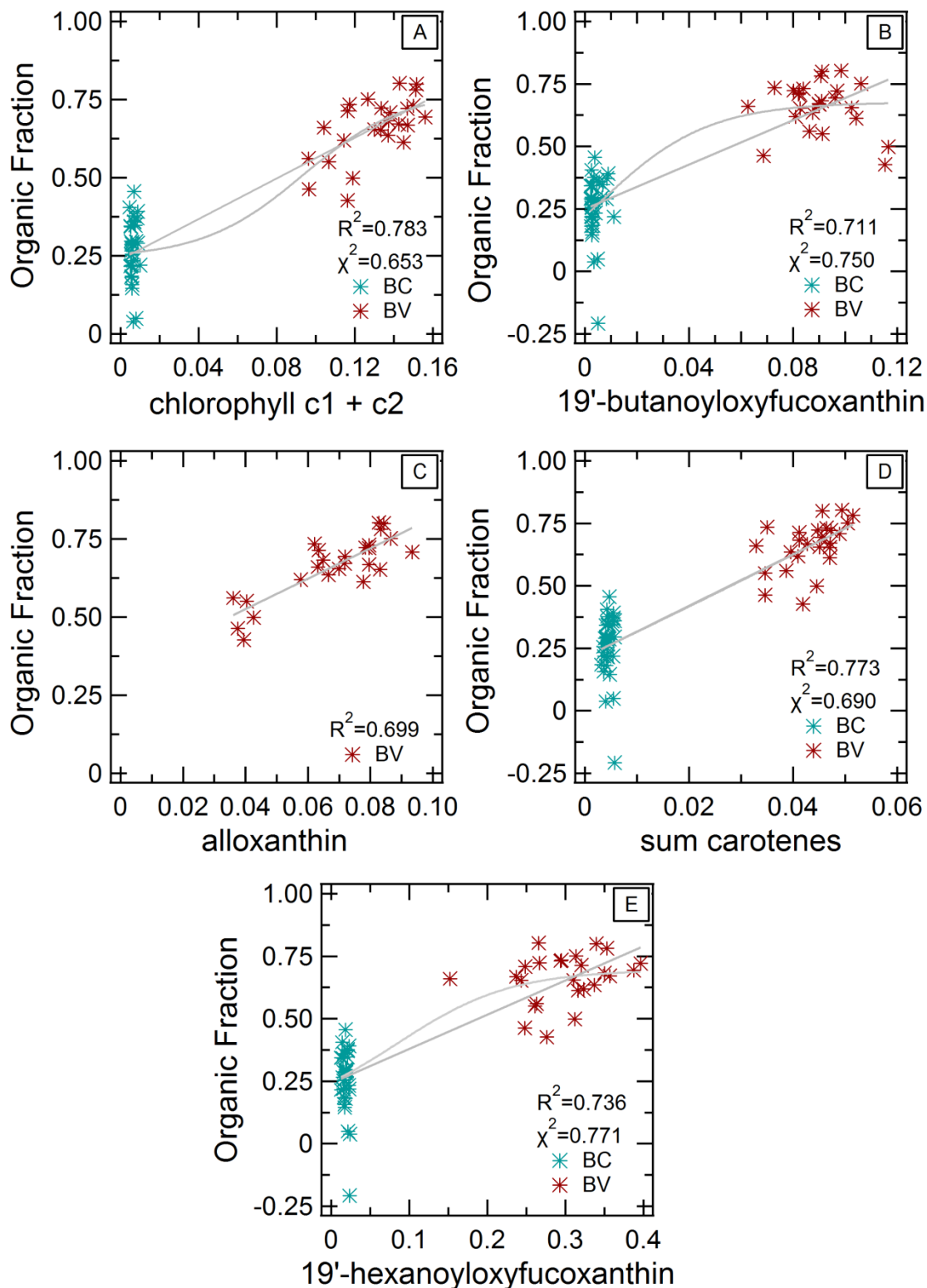
1044



1045

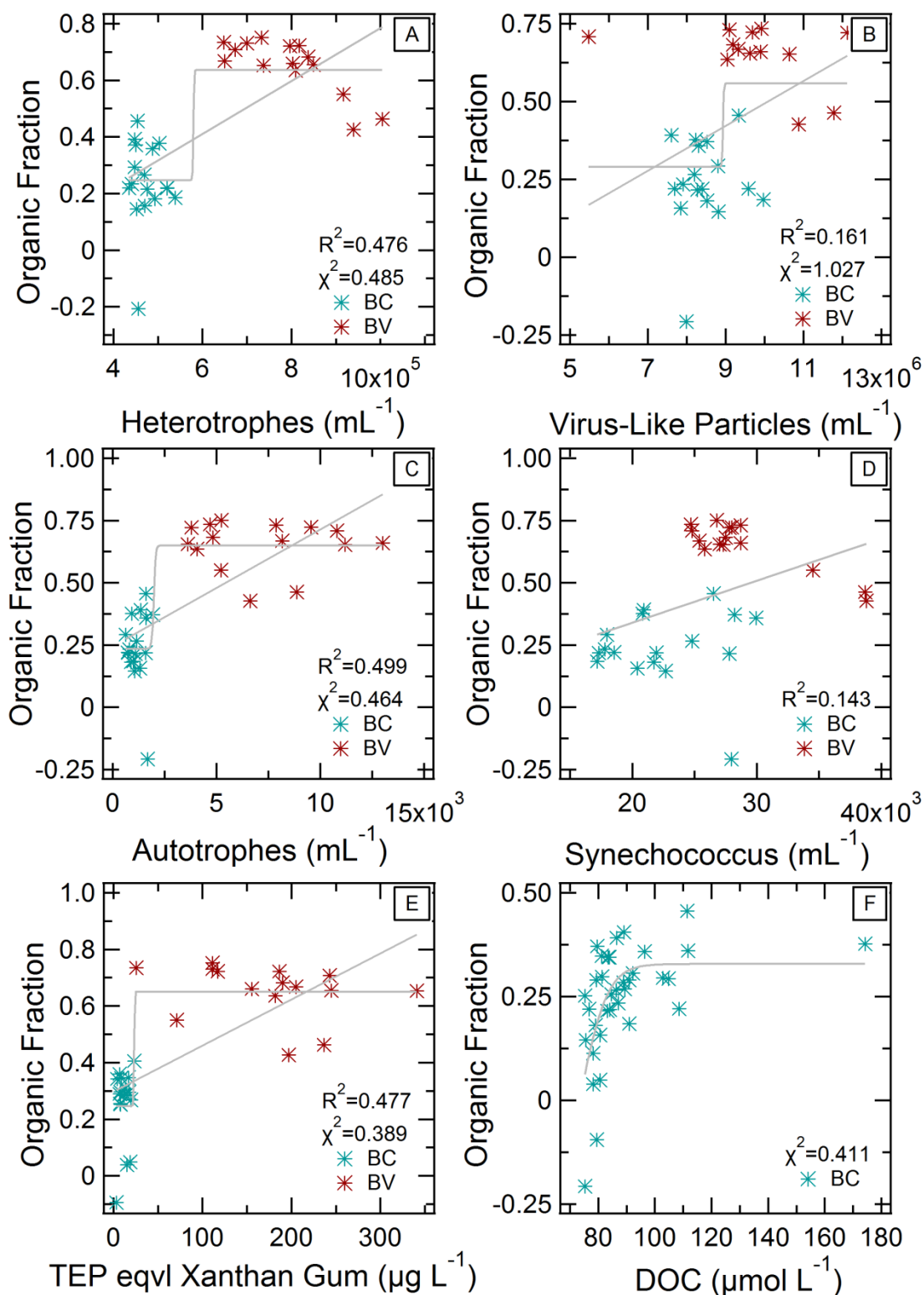
1046 Figure 7. Organic fraction calculated from kappa ( $\kappa_{\text{org}}=0.006$  and  $\kappa_{\text{inorg}}=1.25$ ) at SS=0.39% vs.  
 1047 total chlorophyll-a concentrations ( $\text{mg m}^{-3}$ ) for all 3 mesocosms during both BC and BV, fit  
 1048 with published parameterizations of the organic fraction-chla relationship.

1049



1050

1051 Figure 8. Organic fraction calculated from kappa ( $\kappa_{\text{org}}=0.006$  and  $\kappa_{\text{inorg}}=1.25$ ) at SS=0.39% vs.  
 1052 chlorophyll c1+c2 (A), 19'-butanoyloxyfucoxanthin (B), alloxanthin (C), sum carotenes (D)  
 1053 and 19'-hexanoyloxyfucoxanthin (E) concentrations ( $\text{mg m}^{-3}$ ) for all 3 mesocosms during  
 1054 both BC and BV. Linear fits with R<sup>2</sup> values are shown for all figures, and sigmoid fits with  $\chi^2$   
 1055 values are shown for all panels except for (C).



1056  
 1057 Figure 9. Organic fraction calculated from kappa ( $\kappa_{\text{org}}=0.006$  and  $\kappa_{\text{inorg}}=1.25$ ) at SS=0.39% vs.  
 1058 heterotrophic prokaryotes (A), virus-like particles (B), autotrophic prokaryotes (C), and  
 1059 *Synechococcus* (D) abundances, and TEP equivalent (xanthan gum) (E), and DOC (F)  
 1060 concentrations for all 3 mesocosms during both BC and BV. Linear fits with  $R^2$  values are  
 1061 shown for all figures except for (F), and sigmoid fits with  $\chi^2$  values are shown for all panels  
 1062 except for (D).